TIEGeR: An Energy-Efficient Multi-Parameter Geographic Routing Algorithm

Ishaan Bir Singh

Department of Electrical and Computer Engineering

McGill University

Montreal, Canada

March 2012

A thesis submitted to McGill University in partial fulfillment of the requirements for the degree of Master of Engineering.

ABSTRACT

Geographic routing algorithms conventionally use one-hop greedy forwarding as their primary routing technique, which might lead to routing voids. Secondary routing schemes used to circumnavigate such routing voids are unfortunately not efficient in terms of throughput and energy consumption. Moreover, node residual energy and link quality are not considered during the routing process. This thesis presents a Two-hop Information based Energy-efficient Geographic Routing (TIEGeR) scheme to achieve effective energy balancing throughout the network, while preventing routing voids by proactively avoiding "local maxima" nodes. Distance to reach destination, node connectivity, link quality, and node residual energy are employed to formulate the routing metric for the TIEGeR. Besides, secondary routing scheme dealing with routing voids is supplemented by the reverse progress mode. The proposed TIEGeR algorithm is implemented and evaluated in an IEEE 802.15.4 environment using both simulation based on NS-2 and experimental testbed based on TI CC2530ZDK nodes. Simulations are used to investigate the performance of TIEGeR in large-scale network topologies. By experiment, we further evaluate and demonstrate the real-life operation and performance advantages of the TIEGeR scheme implemented in the network layer of a WSN using IEEE 802.15.4 MAC/PHY layers. Simulation and experimental results verify the advantages of TIEGeR against conventional geographic routing schemes.

ABRÉGÉ

Les algorithmes de routage géographique utilisent conventionnellement des techniques avides de renvois à un bond comme leur technique primaire de routage mais ces techniques peuvent aboutir à une impasse. Les techniques secondaires de routage utilisées pour contourner les impasses ne sont malheureusement pas efficaces en termes de débits ou de consommation d'énergie. De plus, l'énergie résiduelle des nœuds et la qualité des liens ne sont pas considérés durant le procédé de routage. Ce mémoire présente une technique de routage géographique écoénergétique (TIEGeR) à deux bonds et basée sur de l'information pour obtenir un équilibre d'énergie efficace à travers le réseau tout en évitant les impasses en empêchant de manière proactive les nœuds maximaux relatifs. La distance pour atteindre la destination, la connexité des nœuds, la qualité des liens, et l'énergie résiduelle des nœuds sont utilisés pour formuler la mesure de routage pour TIEGeR. Par ailleurs, les techniques secondaires de routage traitant les impasses sont complémentées par le mode de progrès inverse. L'algorithme TIEGeR proposé est implémenté et évalué dans un environnement IEEE 802.15.4 en utilisant des simulations basées sur le NS-2 and en utilisant un banc d'essai basé sur les nœuds TI CC2530ZDK. Les simulations sont utilisées pour examiner la performance de TIEGeR dans une topologie de réseaux à grande échelle. Avec le banc d'essais, nous examinons et nous démontrons le fonctionnement et la performance réalisable de la technique TIEGeR quand elle est implémentée dans la couche réseau d'un réseau de capteurs sans-fil qui utilise la couche physique et la couche de contrôle d'accès au support (MAC) du IEEE 802.15.4. Les résultats des simulations et du banc d'essai vérifient les avantages du TIEGeR contre les techniques conventionnelles de routage géographique.

ACKNOWLEDGEMENTS

First and foremost, I would like to express my deepest gratitude to my supervisor, Prof. Tho Le-Ngoc, for his invaluable advice, motivation and guidance throughout my graduate studies at McGill University. His unconditional support and constant encouragement were vital for me, without which, this thesis would not have been possible. I learnt a great deal, both as a researcher and as person, while working under his able supervision.

I am grateful to Dr. Quang Dung-Ho for his patience and valuable comments that always helped me sail past those difficult situations with ease. I sincerely thank all my fellow lab mates in the Broadband Communications Research Lab for the wonderful discussions, making my stay in the lab a memorable one. Furthermore, I would like to extend my heartfelt gratitude to Ali, Wadood, Haani, Soham and Rashid for all the help and patience during the courses at McGill. Also, a big hug to all my friends I met during the past 2.5 years, especially Ajay, Gautam, Haani, Raffey, Malik, Kumail, Vikrant and Ali, for their unconditional friendship and memorable times.

Finally and most importantly, my deepest love and gratitude is devoted to my parents and brother, who give meaning to my life. To them, I dedicate this thesis.

TABLE OF CONTENTS

LIST OF FIGURES

LIST OF TABLES

LIST OF ACRONYMS

WSNs	Wireless Sensor Networks
GPS	Global Positioning System
UWB	Ultra-Wideband
DSR	Dynamic Source Routing
AODV	Ad hoc On-Demand Distance Vector
TIEGeR	Two-Hop Information based Energy-efficient Geographic Routing
IEEE	Institute of Electrical and Electronics Engineers
MAC	Medium Access Control
PHY	Physical
NFP	Nearest Forward Progress
DREAM	Distance Routing Effect Algorithm for Mobility
LAR	Location-Aided Routing
GEDIR	Geographic Distance Routing
GFG	Greedy-Face-Greedy
GPSR	Greedy Perimeter Stateless Routing
GEAR	Geographic and Energy Aware Routing
EAGR	Energy Aware Geographic Routing
PRR	Packet Reception Ratio
DRE	Density Ripple Exchange
GRR	Geographic Ripple Routing
NIGRA	Neigobors Investment Geographic Routing Algorithm
PATN	Planarization Algorithm based on 2-hop Neighbours
dB	Decibel

TI	Texas Instruments
NS-2	Network Simulator (Version 2)
UDP	Unit Datagram Protocol
LR-WPAN	Low Rate Wireless Personal Area Network
ISM	Industrial, Scientific, Medicine
MHz	Megahertz
GHz	Gigahertz
kbps	Kilobits Per Second
AES	Advanced Encryption Standard
ED	Energy Detaction
CCA	Clear Channel Assessment
LQI	Link Quality Indication
SNR	Signal to Noise Ratio
CSMA-CA	Carrier Sense Multiple Access with Collision Avoidance
PN	Pseudo-random Noise
O-QPSK	Offset Quadrature Phase Shift Keying
DSSS	Direct Sequence Spread Spectrum
BPSK	Binary Phase Shift Keying
SSCS	Service Specific Convergence Sublayer
CTS	Clear-To-Send
RTS	Request-To-Send
GTS	Gauranteed Time Slot
CFP	Contention Free Period
CRC	Cyclic Redundancy Check
FFD	Full Function Device
RFD	Reduced Function Device

PAN	Personal Area Network
CBR	Constant Bit Rate
FTP	File Transfer Protocol
TCP	Transmit Control Protocol
NWK	Network
MSDU	MAC Service Data Unit
PSDU	Physical Service Data Unit
PPDU	Physical Protocol Data Unit
PPS	Packets Per Second

LIST OF SYMBOLS

$d_{i,j}$	Distance between current node *i* and candidate node *j*.
d_0	Reference distance for the log normal shadowing model.
$L(d_{i,j})_{dB}$	Propagation loss over the link between nodes *i* and *j*, measured in dB
$L(d_0)_{dB}$	Propagation loss at reference distance d_0.
γ	Path loss exponent.
X_{dB}	Log-normal shadowing exponent with zero mean and σ^2 variance.
$p_{i,j}$	Link quality index value between nodes *i* and *j*.
N_i	Set of number of neighbours of node *i*.
N_i^{FP}	Set of number of forward progress neighbours of node *i*.
N_i^{RP}	Set of number of reverse progress neighbours of node *i*.
d_j	Distance between node *j* and destination node.
d_i	Distance between node *i* and destination node.
c_i	Normalized connectivity index value for node *i*.
$\overline{E_i}$	Normalized node residual energy level of node *i*.
E_i	Residual energy level of node *i*.
E_{max}	Maximum energy level of a sensor node.
$w_{i,j}$	Value of proposed multi parameter routing metric, applied on current node *i* and candidate node *j*.
α	Weight parameter of the link quality term in the routing metric $w_{i,j}$.
β	Weight parameter of the node connectivity term in the routing metric $w_{i,j}$.
δ	Weight parameter of the normalized residual energy term in the routing metric $w_{i,j}$.

arg	argument.
max	maximum.
j^*	The chosen next-hop node from the set of candidate nodes N_i.
$\lvert\ .\ \rvert$	The cardinal number operator.

Chapter 1

Introduction

1.1 Motivation

Ad hoc wireless networks can function without the support from any pre-existing wired infrastructure, and thus can be deployed in both planned as well as arbitrary topologies. One of the highlight of such ad hoc networks is their ability to self-configure itself to form multi-hop or single-hop communication paths among the nodes in the network. The development of low-cost sensing equipment coupled with such ad-hoc network approach led to the emergence and widespread acceptance of Wireless Sensor Networks (WSNs) for networks comprising of wireless nodes, both fixed as well as mobile. Another important reason for the popularity of WSNs is their self-organizing behavior, reducing the need for human interference for the deployment, maintenance and operation of sensor nodes. In principle, these WSNs help form a bond between the human and the physical entities to setup the *Internet of things*.

WSNs have been successfully employed in a wide array of fields including military, civilian, industrial, commercial and scientific applications [1]. Some of the common applications include disaster management [1], flood detection [1], wildlife tracking and monitoring [2, 3], battlefield support and enemy intrusion detection, resource management [4, 5] etc. More recently, WSNs have been developed for E-Health Systems based on wireless body-strapped medical sensor devices [6, 7]. WSNs have also shown immense potential in the development of smart meters for the administration, monitoring and control of the smart grid [8, 9]. Based on the application, WSNs can have significantly different infrastructure and architectures. Some of the primary characteristics of WSNs are stated below:

- *Scalability*: Depending on the application and the coverage area for the deployment of the WSNs, the number of sensor nodes required to

effectively cover the area could be very large. Such large-scale deployment requires the network to be scalable, i.e., the number of nodes in the network should not affect the self-organizing operational capabilities of the network substantially.

- *Resource constrained sensor nodes*: WSN nodes are typically made up of tiny low-power battery operated sensor nodes. To enable such nodes to operate unattended in remote areas for a long duration of time, the protocol design and the system architecture needs to address energy efficiency concerns by minimizing battery consumption to increase the effective operational lifetime of the entire network. Moreover, WSN nodes have scarce memory and computational capabilities for the protocol and application software implementation. Thus, the protocol implementation has to be concise and simple to enable it to run seamlessly with the limited processing capacity of the nodes, and yet be able to spare enough resources for the necessary buffers and application processes.
- *Communication Model*: One of the key differences between WSNs and the traditional ad hoc networks is the communication model. Ad hoc networks generally communicate using the peer-to-peer model, wherein any node can be the source or destination of the data being transferred in the network. On the contrary, WSNs have dedicated data collection nodes, also referred to as data sinks. Thus, the data traffic often flows from the number of sensor nodes in the network towards these sink nodes designated to collect and process the sensed data from a single or multiple sources. This typically depicts a multipoint-to-point communication model. Depending on the application, there can be one or more sink nodes, but the number is considerably smaller than the number of sensor nodes relaying their information towards the sinks.
- *Delay Constraints*: For certain applications, the freshness of the sensed data is an important constraint. If a node misses these time constraints to report certain critical or emergency situations, the sensed data may be of little significance to the application.

- *Data driven operation*: The individual node address in WSN nodes is not necessary, as they are used only to sense the physical entities around them. The addressing in sensors is achieved by coupling the nodes to their roles or geographic locations. This way, the sensing is done based on specific characteristics, and the sensors that match the specified characteristics report their sensor information towards the sink.

This thesis aims to study and develop an energy efficient and robust geographic routing algorithm for WSN. Keeping in mind all the characteristics of the typical WSN environment, we choose geographic routing as a promising scheme that helps meet the basic requirements of the typical WSN setup. Geographic routing was developed to overcome some of the shortcomings of pre-existing routing schemes vis-à-vis Dynamic Source Routing (DSR), Ad hoc On-Demand Distance Vector (AODV) Routing, Shortest Path Routing Algorithm etc. Most of these existing schemes were stateful and reactive in nature, requiring the global picture of the entire network for routing decision making. This induced large quantities of overhead before the actual data could be routed towards the destination. Being stateful, such algorithms are highly vulnerable to mobility of nodes, as any change in the network topology requires reconfiguration of the routes inducing more overhead message costs. Geographic routing uses node's position information to navigate the packet towards the designated destination. Geographic routing is comprised of two complementary routing schemes: greedy forwarding and perimeter routing [10]. The primary routing scheme employed is the greedy forwarding scheme, wherein a packet is routed to the node that is closest to the destination among all the neighbouring nodes (Figure 1.1). This behavior is continued till the destination is reached or till a *routing void* (no node closer to the destination than the current node itself) is encountered. This node, also referred to as the *deadlock* node, initiates the secondary routing scheme (perimeter routing). Perimeter routing is used to circumnavigate the packet around the routing void till the time the greedy forwarding mode can be re-applied. Being stateless in nature, i.e. not requiring storing the entire path to the destination, the geographic routing reduces a considerable amount of overhead by just considering and storing link

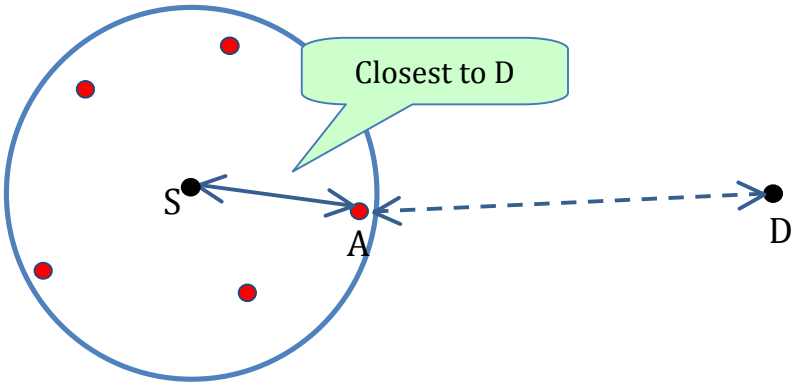

Figure 1.1 Distance Based Greedy Forwarding.

level information (one-hop or two-hop information) for routing purposes. Moreover, being a distributed proactive routing algorithm, the geographic routing algorithm is typically unaffected by the size of the network, making it highly dynamic yet simple to implement and operate. These properties make geographic routing highly suitable especially for resource and energy constrained WSNs [10].

1.2 Contributions

A very attractive observation made during the review of the existing geographic routing protocols was that most of the research was focused on 1-hop neighbourhood information based routing schemes, which often leads to very limited information for packet traversal, consequently resulting in routing voids. Motivated by this, we explore a modified geographic routing algorithm utilizing 2-hop neighbour information to route the packets towards the destination. This thesis focuses on devising a new geographic routing algorithm named TIEGeR (Two-Hop Information based Energy-efficient Geographic Routing) that makes the best use of the additional neighbours' information. In order to further strengthen the proposed scheme, we aim to address other relevant limitations of sensor nodes including limited energy resources, effect of environmental and physical limitations like link quality degradation due to propagation losses and the

effect of density onto the network dynamics. The metric proposed in this thesis combines the effects of multiple network and node parameters like current node geographical location, node connectivity information, residual energy level and link quality, to aid in a better routing decision with the aim of avoiding the deadlock situations in an energy efficient fashion. The proposed TIEGeR algorithm employs different combinations of the network parameters for the two hops being studied. For the first hop, a combination of link quality, geographic distance and node residual energy is used. For the second hop, a simple node-connectivity based model is utilized. This leads to improved efficiency and reduced metric decision computational time. This is primarily due to the reduced second-hop computational complexity by using only the connectivity factor for the second hop. The contributions of the proposed scheme are as follows:

- Dedicated secondary routing algorithm is not required. Instead, TIEGeR initiates its *reverse progress mode*, where packets are still forwarded in a greedy fashion using the proposed routing metric.
- The proposed multi-parameter based routing metric reduces the likelihood of encountering routing voids by using the node connectivity information to forewarn about the local maxima nodes. This leads to the *reverse progress mode* initiated sparingly, thus improving the overall routing efficiency of the TIEGeR.
- By using the node residual energy parameter, the TIEGeR achieves effective and efficient energy balancing throughout the network. This helps prevent the network partition due to battery-depleted nodes.
- Employing link quality as an active element in the routing process ensures that during the course of avoiding routing towards deadlock nodes, the packets are still forwarded to nodes with better link quality.
- The TIEGeR proves its effectiveness in both static and mobile network scenarios. The simulation results illustrate the superior performance of TIEGeR even in mobile networks.

To demonstrate the practical application of TIEGeR, the algorithm is implemented on a WSN testbed. Thus the performance superiority of TIEGeR is realistically verified in the measured results on the experimental testbed. Furthermore, in order to have a more concrete analysis of the results, we undertake the analysis of the IEEE 802.15.4 Medium Access Control (MAC) and Physical (PHY) layers in order to identify the performance constraints induced by the MAC and PHY sublayer functionalities. This helps isolate the effect of the routing protocol onto the evaluation parameters used to test comparable routing algorithms.

1.3 Thesis Organization

The rest of the thesis is organized as follows. A literature review of the traditional and recently proposed geographic routing algorithms is presented in Chapter 2. Chapter 3 deals with the various aspects of the proposed TIEGeR Algorithm. The chapter begins with the description of the routing parameters being considered in TIEGeR followed by the new 2-hop neighbourhood information based multi-parameter routing metric. Further, the steps involved in the protocol design are discussed. It also includes the implementation details regarding TIEGeR and the operational parameters for the simulation as well as the experimental testbed setup used for the analysis of the TIEGeR algorithm. The chapter concludes with a series of operational validation tests for TIEGeR. In Chapter 4, a thorough evaluation of the TIEGeR algorithm is presented based on the simulation and experimental results highlighting the advantages of TIEGeR algorithm both in simulation based complex network topologies and experimental testbed based real-world deployments. The chapter begins with a study of the effect of environmental factors on the 802.15.4 MAC and PHY layers to identify the operational threshold of the experimental testbed used for the evaluation of the proposed routing protocol. This is closely followed by the analysis of the network layer using a mix of simulation and measurement based analysis. The network layer analysis is based on complex network scenarios implemented to highlight

the importance of individual routing parameters considered in the routing metric. For each network scenario, a mix of large-scale simulation setup based results is followed by a relatively simpler and small-scale measurement results from the experimental tested. Finally, Chapter 5 concludes the thesis.

Chapter 2

Geographic Routing: A Review

Geographic routing is a node position based routing technique that delivers a message utilizing a single hop/multiple hops towards the destination node. Geographic routing is a distributed routing algorithm eliminating the need for routing tables or route discovery activities. These fundamental properties make geographic routing attractive for dynamic networks such as wireless ad hoc and sensor networks. Thus, geographic routing algorithms are nearly stateless and deliver high packet success rates with relatively much less network overhead as compared to more complex centralized routing algorithms.

The prime assumptions considered by geographic routing algorithms are as follows:

- A node can determine its own position.
- A node is aware of its neighbours' positions.
- The position of the destination is known.

For the first assumption, low-cost and low-power GPS or similar navigation systems can be used to deliver current position information to the wireless nodes. Broadcasting the updated position information periodically to the neighbouring nodes in the network fulfills the second assumption. With this information a node is able to determine the next-hop that is closer to the destination. The third assumption can be met by means of a location service that spreads out periodic update regarding the position of the destination node into the network. In some cases, the destination is inherently known to the nodes, e.g., in some sensor network applications where a single sink node collects all the data measurement information.

The key necessity to meet the above stated assumptions is a reliable and efficient node position tracking system. However, a simple greedy forwarding scheme minimizing the distance to the destination in each step cannot guarantee message delivery. As stated earlier in the previous chapter, this might lead to situations where no neighbour is closer to the destination than the current node. Greedy algorithms cannot resolve such deadlock or local maximum situation. Therefore, recovery methods have been developed, the most prominent of which are based on face routing, where the message is navigated around the deadlock by traversing the edges of a planar sub-graph of the network. Planar graph routing techniques can provide delivery guarantees under certain assumptions and complement the efficient greedy forwarding schemes. This chapter gives an overview of geographic routing starting with greedy algorithms and face routing based recovery strategies in Sections 2.1.1 and 2.1.3, respectively. Section 2.1.4 discusses the combined greedy and face routing algorithms. Section 2.2 describes node residual energy based geographic routing schemes as an energy aware variant of geographic routing. In Section 2.3 algorithms and methods for geographic routing under realistic network models are reviewed. Further node connectivity aware variants for geographic routing are described in Section 2.4. Finally, Section 2.5 explains various two-hop neighbour information based geographic routing algorithms in the literature.

2.1 Geographical Routing Techniques

2.1.1 Simple Greedy Forwarding

Geographic routing belongs to the broad domain of position based routing algorithms, wherein a node's location information is used to route the packet towards the destination node's location. Utilizing node position information for routing purposes was first proposed in 1984; mainly for packet radio networks and other wired networks [11]. The proposal was to make locally optimal decisions to select the next-hop node based on the position information of the candidate nodes. Thus, the distance based forwarding approach selected the next-

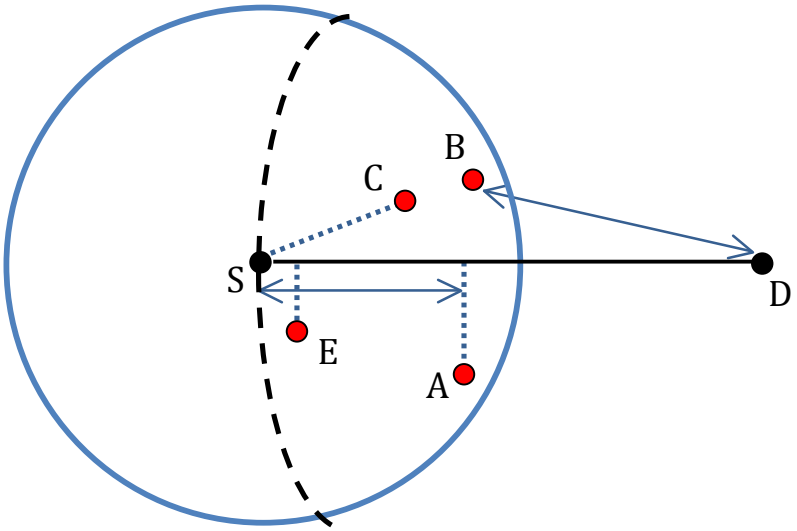

Figure 2.1 Greedy Forwarding Strategies.

hop node based on the maximum distance progress towards the destination area. This concept of progress has been defined as the projection of the candidate node on the line joining the packet source node and the destination node (Node A in Figure 2.1). The most popular mechanism used is the greedy forwarding scheme where the next-hop is chosen in such a way that the packet is propagated closer to the destination node in every hop/step. This behavior is continued until the packet reaches the destination node or is unable to forward the packet using the simple greedy principle. Some popular greedy forwarding schemes are shown in Figure 2.1 [18].

Node A refers to the notion of progress. Packet progress refers to the projection of node A onto the line joining the source node S and the destination node D (line SD in the Figure 2.1). Node B belongs to the typical distance-based greedy forwarding scheme, wherein the aim is to minimize the Euclidean distance between the selected next-hop node (node B in Figure 2.1) and the destination node D. Node C depicts another class of greedy forwarding schemes that focus of direction-based greedy forwarding. In this scheme, the angle formed by the current node, the next-hop node and the destination node is the selection criteria for routing. Thus, as seen in Figure 2.1, node C minimizes the angle formed by the next-hop node and the destination node D. Such scheme is also referred to as

Compass Routing protocol. Node E illustrates the Nearest Forward Progress (NFP) routing scheme. In this scheme, the aim is to minimize energy consumption by adjusting the transmission range and choose the node closest to the current source node S, still being closer to the destination node as compared to the current source node S. In other words, the NFP routing scheme chooses the node among the Forward Progress nodes that is closest to the current node S. This scheme is very effective in highly dense network topologies, where the nodes are closely spaced, thus more options for NFP to forward the packet. Selecting the next-hop by the minimum distance or the maximum progress gives an inherently loop-free forwarding rule independent of the unit disk graph assumption. Compass routing, which is based on the direction, is not loop-free. In Hybrid Geographic Routing (HGR) [12], a flexible routing scheme is presented that uses a combination of distance-based and direction-based forwarding strategies. HGR selects the next hop with large distance progress and small deviation angle. A weighting factor is used to achieve a flexible tradeoff between distance and direction based strategies in order to minimize the energy consumption and the packet latency. Using the proposed Dynamic HGR (DHGR) node weight adjustment mechanisms, the overall QoS requirements in terms of end-to-end packet delay and energy savings are fulfilled by ensuring that the localized per-hop forwarding decisions meet the latency and energy constraints presented by the global QoS requirements.

Extensions to the traditional geographic forwarding schemes have been proposed that take into account node mobility. In the next subsection, we discuss a few advanced geographic routing schemes; including node mobility based routing schemes.

2.1.2 Advanced Strategies

The first advanced geographic routing strategy is the Distance Routing Effect Algorithm for Mobility (DREAM) protocol [13]. DREAM broadcasts location updates based on the distance of the packet from the packet destination and the speed of the mobile node. In DREAM, every node maintains a location table storing the current position of all the neighbouring nodes. Based on this update of

the current position of the one-hop neighbours, all the one-hop neighbours in the direction of the receiver are identified. Hereafter, the routing is done by sending the data packets to the one-hop neighbours that are currently located in the direction of the receiver. Thus, location management and update constitutes an important part of the successful routing decision. In the location management, there are two primary observations that control the location updates. Firstly, the greater is the distance between a given point and a node, the slower the node seems to move. Thus, the location updates have to travel longer distances less frequently. To implement this, a lifetime is assigned to the location updates. Now, for the frequent updates, the lifetime will be shorter, whereas for less frequent updates, he lifetime will be longer, allowing them to travel longer distances.

Another significant geographic routing protocol worth discussing is the Location-Aided Routing [14] (LAR). LAR is a *reactive routing protocol*, using the location information for route discovery instead of routing of data packets. For each node LAR defines an expected zone and a request zone. As the name suggests, the expected zone refers to the area where a node is supposed to be located based on its last known position and speed. The request zone is the area where the neighbour nodes perform route discovery locally. LAR has two schemes of operation. In LAR scheme 1, the request zone is a rectangle, which starts from the node initiating the query (usually located at a vertex), and extends through the entire expected zone (usually the vertex opposite to the query initiator vertex). Inside this defined request zone, any intermediate node receiving the query either forwards it further or discards it. However, in LAR scheme 2, any intermediate query forwarder within the request zone forwards the packet only if its location provides some advancement to the expected zone.

Greedy forwarding has one important drawback: it fails in *local maximum* situations where the forwarding node has no other neighbours closer to the destination. Under these circumstances, some cases require a sophisticated strategy to recover from this situation; in other cases, a simple backward step is

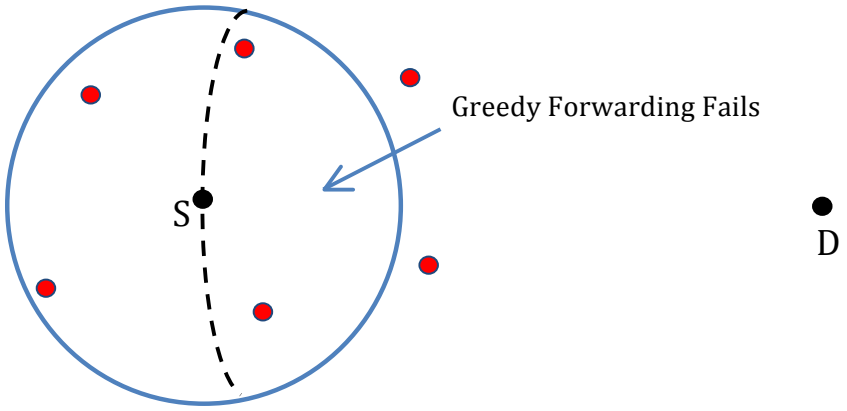

Figure 2.2 Greedy Forwarding Failure Scenario.

sufficient to be able to resume the greedy strategy successfully. The Geographic Distance Routing (GEDIR) [16] method is such a greedy strategy with backward steps. Whenever a message has reached a local maximum, the packet is sent back to the previous hop, which applies the greedy rule again while excluding previously visited dead-end nodes from the routing decision. This strategy is also loop-free.

2.1.3 Face Routing

Planar graph based routing [17] is a geographic routing strategy that is able to overcome the local maximum problem of greedy forwarding. It is based on the concept that the network links form a communication graph, and a message can be routed along a sequence of faces in this graph. Routing along a face means that the nodes of a face pass the message along the incident edges by locally applying the left-hand or right-hand rule (see Figure 2.3). This rule is well-known from maze problems: One can find a way out of every simply connected maze when having the right-hand always in touch of the wall while walking. Applying the right-hand or left-hand rule to network graphs results in the traversal of a face of the communication graph. For a successful application of this rule, the underlying graph has to be planar. Face routing is one of the most widely used recovery strategy to counter the routing void problem in traditional greedy forwarding.

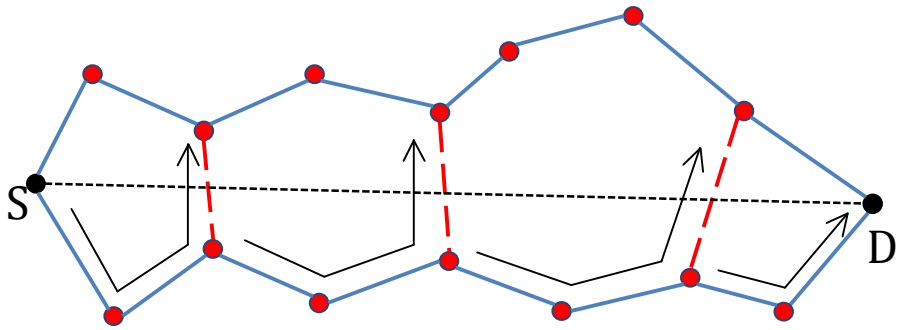

Figure 2.3 Face Routing.

2.1.4 Combined Greedy and Face Routing Schemes

The planarity of the underlying network graph is required for assuring delivery guarantees, because crossing links as shown in Figure 2.3 can cause detours or routing loops. Therefore, an arbitrary unit disk graph has to be transformed into a planar graph first. The removal of edges however can increase the hop count, which makes face routing less efficient than greedy routing. Therefore, in Greedy-Face-Greedy (GFG) Algorithm [17] a combination of efficient greedy forwarding and face routing on a planer subgraph as a recovery mechanism from local maxima was proposed. This scheme was further strengthened in Greedy Perimeter Stateless Routing (GPSR) [10].

Both GFG and GPSR use greedy forwarding as long as possible. If greedy routing fails, a face traversal starts until the greedy strategy can be resumed. When starting recovery, the distance of the first node to the target and the first edge is stored in the packet header. If the same first edge is visited again for the second time, then the destination is not reachable and the packet is dropped. The distance is used to check whether the next-hop on the face traversal is closer to the destination than the node entering recovery mode. If such a node is found, greedy forwarding can be resumed instead of continuing the traversal until crossing the line joining the source node and the destination node.

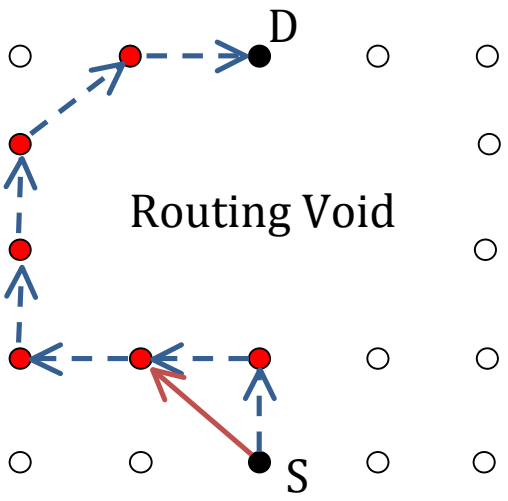

Figure 2.4 Learning Routes around Routing Voids using GEAR.

2.2 Node Position and Energy Based Geographic Routing Techniques

A very important limitation of WSNs is the nodes' limited energy resources. Hence, energy efficiency becomes a prime concern to be addressed by the algorithm design. This is a major drawback of conventional distance based geographic routing protocols. Due to the lack of energy aware routing metrics,

these conventional geographic routing schemes tend to overuse the battery resources among the static path chosen by the algorithm, thus leading to network portioning due to nodes powering out on these excessively used paths towards the destination. To overcome this typical drawback of geographic routing algorithms for WSNs, energy aware routing metrics have been proposed in the literature that take into account the residual battery levels of the nodes in order to account for a more evenly distributed energy depletion trend among all the nodes in the network. One of the first geographic routing scheme incorporating node residual energy levels for routing purposes was Geographic and Energy Aware Routing Protocol. In GEAR [19], a distance and residual energy based routing protocol to route around voids is proposed. Using a combination of estimated cost and learned cost of reaching the destination through its neighbours, each data packet is dissipated though the network towards the destination. The estimated cost is a

combination of residual energy and distance to destination. The learned cost is a refinement of the estimated cost that accounts for routing around holes in the network. There are two phases in the algorithm. The first phase comprises of the distance and node energy based greedy forwarding technique to forward the packet closer to the destination region. In the second phase, the packet is diffused in the target region either by recursive geographic forwarding or restricted flooding.

HobyCan [20] presents another location and residual energy based scheme that constructs multiple paths for packets. This, in turn, distributes the load onto the alternate paths around the hole, thus preventing fast depletion of nodes around the routing void. HobyCan protocol addresses the load balance among nodes, especially ones on the boundary of hole, by constructing multiple detour paths around a hole. To prevent exhausting of detour nodes, a threshold *E_THR* is specified, below which the node ceases to work as detour node. HobyCan starts with greedy forwarding and turns to perimeter mode when a local maximum node (detour node) is approached, wherein packets are routed using multiple detour paths around the hole rather than a single path.

Energy Aware Greedy Routing (EAGR) [21] is another energy based geographic routing scheme where a cost metric based on distance, fraction of energy consumed and rate of energy consumption is presented. The aim of using the rate of energy consumption is to improve energy consumption of the nodes. Each node advertises its location, fraction of energy consumption and the rate of energy consumption using a periodic beacon exchange protocol. These values are used to update the neighbour table of all the direct neighbour nodes receiving the broadcasted beacon message. Now using the proposed cost computation metric, EAGR chooses the node among the neighbours closer to the destination and returning the least value of the cost computation parameter. In other words, the next-hop is chosen that is closer to the destination and has the least value for the routing metric.

Another Energy-efficient and QoS-aware Geographic Routing (EQGR) technique was recently proposed in [22]. In EQGR, two separate neighbour tables are maintained at each node for the reliability and real-time domains. The EQGR algorithm aims to minimize the latency, missed-deadline delivery and control message overheads while achieving reliable data forwarding by employing energy-efficiency and link quality during the routing process to maximize the network lifetime. In the real-time domain, EQGR assigns different end-to-end deadlines to each packet based on the different level of importance of each data packet. Moreover, in the reliability domain, link quality information is used to improve the success probability of the packet. To achieve this, EQGR computes optimal forwarding node using the information regarding the residual energy level, occupied buffer level, link quality and the required energy for packet transmission for each candidate node.

Energy-aware Multipath Geographic Routing (EMGR) [23] is another multiple forwarding path based energy-efficient technique utilizing geographical location information, energy consumption characteristics and proposes advanced energy cost metrics to select the next hop node. In order to maximize the network lifetime, the nodes in EMGR adjust their transmission power level to reach the selected forwarding node. In case of the secondary routing mode, EMGE uses a dynamic anchor list in order to shorten the routing path. Thus, both during the primary greedy forwarding and the secondary detour modes, using different optimal anchor nodes and intermediate forwarding nodes for different packets constantly varies the routes. This minimizes the total energy consumption of the network, thus prolonging the network lifetime.

2.3 Position and Link Quality Based Geographic Routing Techniques

The distance based greedy forwarding techniques in Section 2.1 and the energy aware algorithms in Section 2.2 assume a simplified binary link layer model, where the radio range is mapped as an ideal sphere. However, the validity of this

idealized assumption has been challenged in many research studies [24, 25, 26]. Choosing the next-hop closest to the destination node may lead to poor link quality because of the increased distance between the sending and the receiving nodes. The product of link quality, measured as Packet Reception Ratio (PRR) and distance from destination has been shown to be a good routing metric for geographic routing [26]. [26] utilizes a realistic link loss model, where the reception region is divided into three regions – connected, transitional and disconnected. Also, [26] uses a log-normal shadowing based link loss model to demonstrate the lossy links in a realistic environment. By blacklisting the links with low PRR, he routing scheme avoids links with lower link quality, thus increasing the throughput of the network. Key results and mathematical analysis show that the common greedy forwarding approach would result in very poor packet delivery rate. Efficient forwarding strategy (*PRR*D*) takes advantage of links in high variance transitional region both for energy efficiency and to minimize route disconnections. The *PRR*D* metric is recommended for static or low dynamic environments, as for highly dynamic environments, the PRR estimates become difficult.

More recently, a weighted sum of *PRR*D* product along with the node residual energy has been shown to achieve higher network lifetime [27, 28]. In this algorithm, the typical *PRR*D* model described above is coupled with the residual energy level of the node by taking a weighted sum of *PRR*D* and the node residual energy. This way, the nodes with low residual energy levels are avoided while routing packets using good quality links. This helps improve the overall network lifetime of the network.

2.4 Position and Connectivity Based Geographic Routing Techniques

In [30], Li presents a distance and node connectivity based geographic routing scheme. The routing metric comprises of a weighted sum of the distance from destination and the connectivity factor, computed over all the neighbourhood

nodes to choose the next-hop. A new routing protocol, Density Ripple Exchange (DRE) that maintains local density information at each node, and a new geographic routing algorithm, Geographic ripple routing (GRR), that achieves better routing performance by exploiting available connectivity information, is presented in [21]. The GRR algorithm is based on the Ripple function, which presents the connectivity model for the algorithm. Nodes close to void area or on the edges of the void area have less neighbour density. Also, nodes isolated with their neighbours have less neighbour density. Based on this, it is intuitively believed that nodes with low neighbour density are likely to lead to stuck position. Thus, to avoid nodes around the void areas, the beacon messages exchanged by the nodes also contain the connectivity information along with the location information of nodes. On receiving a beacon message, a node extracts the geographic and connectivity information and applies to the ripple function to decide next node. A node with less neighbour density will introduce large ripple. Consequently, a node with high density introduces little ripple. With this concept, nodes calculate ripple power depending on their density and send along with beacon message. The routing metric is based on the proximity function that presents a weighted sum of geographic location and connectivity status computed by the ripple function.

2.5 Two-Hop Information Based Geographic Routing Schemes

It has been observed that most of the geographic routing algorithms studied are based on 1-hop neighbourhood information. The possibility of incorporating 2-hop neighbourhood information in the routing decision was proposed in GEDIR-2 [16], which shows that using 2-hop information leads to higher packet delivery rate and shorter hop counts as compared to simple 1-hop Greedy forwarding. In GEDIR-2, the current node chooses node closest to destination among all 1-hop and 2-hop neighbours and forwards the message to its neighbour that is connected to the choice. In case of ties, the algorithm chooses the node that is closest to destination. In simple GEDIR algorithm, the message is dropped in case of a

deadlock situation. To overcome the problem of deadlock, GEDIR-2 proposes flooding as a solution. Flooding is done only at the local maxima node. The rest of the nodes receiving the flooded message packet follow the normal Greedy Forwarding from then on. One of the noteworthy drawbacks in GEDIR-2 is the possibility to always select a node approaching dead-end over the ones that prevent it, as it always selects the best node to be the one closest to the destination among both 1-hop and 2-hop neighbours.

Further, the 2-hop information based approach can also be applied to other basic geographic routing strategies vis-à-vis Greedy, MFR and Compass Routing schemes. In such a scenario, the routing scheme chooses the most suitable node from the 2-hop neighbourhood of the current node. The packet is then forwarded to the neighbour node that is directly connected to the chosen second-hop node by the routing algorithm. The primary advantage of using the 2-hop neighbourhood information lies in the fact that it helps prevent routing the packets towards the deadlock nodes. With the information regarding the 2-hop neighbourhood, the current node has an indication regarding the probable position of the routing void. This is achieved by avoiding the nodes with no 2-hop forward progress neighbouring nodes.

Liu *et al.* [31] present an improved version of GEDIR-2 called Neighbours Investment Geographic Routing Algorithm (NIGRA), which uses only the second hop neighbour location for routing decision. NIGRA adapts NIR (Neighbours Investment Routing) algorithm as primary routing strategy, which makes nodes aware of existence of voids, to aid packets bypassing the dead-end nodes in advance. NIR chooses node closest to the destination among only the second hop neighbours, not both 1-hop and 2-hop neighbours, as in GEDIR-2. In this algorithm, the metric finds second hop neighbour closest to destination, and then searches for the 1st hop node connecting the chosen second hop node and the current node. This helps avoid the limitation of GEDIR-2 as pointed above. NIGRA resorts to perimeter routing in case of deadlock, but uses PATN (Planarization Algorithm based on 2-hop Neighbours) to compute planar graphs

from network topology. This planarization technique uses 2-hop neighbour information to planarize network, and thus avoid extra planarization cost.

In [29], a modified version of PRR*D routing metric is used over k-hops for routing, which shows an improvement in terms of packet delivery rate and hop count as compared to conventional geographic routing algorithms. Firstly, a study of simple geographic greedy routing using k-hop neighbourhood information is presented. It is shown giving examples that the 2-hop case is an efficient way to resolve deadlock situations, by blacklisting the deadlock node and avoiding it as next-hop node. Secondly, a new routing metric incorporating PRR and distance is proposed and generalized for k-hops case. Comparing over increasing number of k (number of hops considered for neighbourhood information sharing), it can be seen that the new metric in [29] performs better as compared to simple greedy based routing. It is found that there is a significant improvement in number of transmissions required from source to sink when multi hop information is used, especially in harsh environments.

It must be noted, though, that for the 2-hop information based routing scheme to function, it requires 2-hop neighbourhood information to be distrusted among the neighbouring nodes. This process of sharing the 2-hop neighbourhood information necessitates an increase the amount of control message overhead for the routing algorithm. A complexity analysis for a network of n nodes was presented in [32], which states that every node can obtain the knowledge of its 2-hop neighbourhood nodes in a total of $O(n)$ messages, each message being $O(\log n)$ bits in size.

A greedy-based algorithm that goes beyond using 2-hop information is SPEED [33]. It uses an additional “backpressure” heuristic to avoid congested areas and void regions. The protocol uses on-demand beacons for delay estimation and backpressure information. Nodes from the greedy area, whose relay speed is above a certain threshold, are selected probabilistically. The higher the relay speed the higher the probability to be selected. If no neighbour meets the relay speed requirement, the node drops the packet with a certain probability that

depends on the failure ratio of packet forwarding to the neighbours. The necessary information to derive the failure ratio is gained from the neighbours by backpressure beacons, which are sent in case of congestion or in a local maximum situation. This method can alleviate local maxima problems in case of small void regions, but it cannot guarantee delivery in general.

Chapter 3

Two-hop Information based Energy-efficient Geographic Routing (TIEGeR): Algorithm and Protocol

This chapter presents the proposed TIEGeR algorithm and its various aspects. We begin with the models adopted for the calculation of packet reception rate, normalized node connectivity, node residual energy and modified beacon mechanism to develop a new routing metric. Section 3.1 presents a brief review regarding the link quality model incorporated into the proposed routing metric. Section 3.2 discusses the node connectivity model used to calculate the connectivity factor of the second-hop neighbour nodes. Section 3.3 deals with the node residual energy model used in calculating the residual energy of all the nodes in the network. This energy model is closely related to the battery drain model presented in Section 3.4. This battery model presents an energy model based on a realistic battery drain characteristics derived from experimental analysis of the Texas Instruments (TI) CC2530 based testbed. Next, in Section 3.5, we discuss the modified beacon exchange protocol, which is an essential part of the TIEGeR algorithm. The modified beacon exchange mechanism carries updated information used by the nodes to ensure correct and efficient routing of data packets. Section 3.6 presents the modified routing metric incorporating the features of all the above-mentioned routing parameters. The TIEGeR algorithm to route the packets towards the destination utilizes this modified routing metric. The steps in the TIEGeR algorithm, along with its implementation details are presented in Section 3.7. Section 3.8 summarizes the simulation and experimental testbed environment parameters and the traffic characteristics. Section 3.9 presents some typical test cases simulated for operational verifications of the proposed TIEGeR Algorithm.

3.1 Link Quality

Link quality is an extremely crucial parameters affecting successful delivery of transmitted packets. Thus, it becomes of paramount importance to take into consideration the link quality between two nodes before choosing the next-hop for the packets being transmitted. This section deals with a link quality model that is simple to compute based on the *long-term path loss* model. [34].

$$L(d_{i,j})_{dB} = L(d_0)_{dB} + 10\gamma \, log\left(\frac{d_{ij}}{d_0}\right) \quad (1)$$

where $L(d_{i,j})_{dB}$ is the average power loss in dB over the link of distance $d_{i,j}$ between nodes *i* and *j*, γ is the path loss exponent, and $L(d_0)_{dB}$ represents the path loss in dB of a close-in distance d_0 taken as a reference. The more the distance between current node *i* and candidate node *j*, higher will be the link power loss, and thus, lower link quality. Based on the path loss model, we present the link quality between two nodes as:

$$p_{i,j} = \left(\frac{d_0}{d_{ij}}\right)^{\gamma} \quad (2)$$

This value of link quality is updated periodically for each pair of current node *i* and host of candidate nodes *j* by using their current location. These location parameters are extracted from the periodic beacon/hello messages and used to compute the distance between the current node and the candidate node. This value of distance is used in equation (2) to get an indication of the link quality over the link joining current node *i* and the corresponding candidate node *j*. The computed link quality estimate is saved in the neighbour information list corresponding to the source of the beacon message. This value is consequently referenced by the routing metric to decide the next-hop node for the packet transmission. This procedure is repeated over all the links in the network to get an estimation of the link quality over all the links in the network.

3.2 Node Connectivity

In this section, a new node connectivity model is presented, which is based on the local connectivity status of a node. Before proceeding further, it is essential to define *connectivity* of a node. In [30], it has been observed that nodes close to the void area or on the edge of the void area have low neighbour density, i.e., the number of neighbourhood nodes in the transmission range of a node. Also, nodes isolated from their neighbours or around the edge of the network topology have low neighbour density. Keeping this in mind, it can be seen that the nodes with low neighbour density are more likely to lead to a deadlock situation as compared to nodes with higher neighbour density. This is due to the fact that nodes with higher density have a higher probability of finding an alternative path towards the destination. Based on the above observation, the connectivity for a given node can be defined as the number of *Forward Progress* neighbours available for the node.

To better understand the *Forward Progress* and *Reverse Progress* neighbours principle, let the set of neighbours of a particular node *i* be denoted by N_i. A *forward progress* neighbour of node *i* is defined as the one that is closer to the destination than node *i*. A *reverse progress* neighbour of node *i* is defined as the one that is farther away from the destination as compared to node *i*. Let N_i^{FP} and N_i^{RP} denote the set of *forward progress* neighbours and the set of *reverse progress* neighbours of node *i*, respectively. In other words, $N_i^{FP} = \{j \in N_i : d_j \leq d_i\}$, $N_i^{RP} = \{j \in N_i : d_j > d_i\}$, and $N_i^{RP} \cup N_i^{FP} = N_i$. Then the *normalized connectivity* of node *i*, denoted by c_i, can be defined as

$$c_i = \frac{|N_i^{FP}|}{|N_i|} \tag{3}$$

where |A| is the cardinal number of set A. This value of the connectivity is then used in the proposed routing metric.

3.3 Node Residual Energy

One of the most prominent limitations of wireless sensor networks is that the sensor nodes have limited energy resources, as these nodes are often battery powered. This, in turn, necessitates the consideration of residual energy level as a contributing factor in the process of data packet forwarding/routing. But before discussing the contribution of the energy model in the routing process, it is essential to have a practical, simple and efficient node residual energy model to keep track of the battery level at all times. This section presents a new energy model that addresses energy limitations of the sensor networks. This model specifically captures the residual energy levels of the sensor nodes as a normalized residual energy model. For each node, the node residual energy is mapped according to the following residual energy model, normalized over the start-up energy level of the nodes, which clearly is the maximum energy level for any node in the network:

$$\overline{E_i} = \frac{E_i}{E_{max}} \tag{4}$$

where, E_i is the residual energy level of node i and $\overline{E_i}$ represents the normalized node residual energy status for node *i,* normalized over the maximum energy level of node, $E_{max.}$ Thus, the higher the value of $\overline{E_i}$ the higher is the node residual energy. For the sake of simplicity, we assume negligible energy consumption during packet processing at the nodes. Thus, the major factors utilizing a node's energy resources are the wireless radio processes of packet reception and packet transmission. Every time a node's radio receives or transmits a packet, a certain amount of energy is consumed, which in turn is reduced from the residual energy level for the node. The updated value at each beacon message interval is exchanged with all the neighbour nodes by sending the updated node residual energy level in the beacon exchange message packet fields.

3.4 Energy Model

To monitor the battery drain characteristics of the sensor nodes, a realistic energy model is required. The energy model currently available in NS-2 [35] is a simplistic model representing the current battery energy level. Each node is initialized with a max-startup energy level. Each time the node transmits or receives a packet; the battery level is decremented by a pre-specified value. A node ceases to transmit/receive any further packets when its residual battery level drops to zero. Even though it is claimed that this model monitors the energy drain characteristics realistically, in practice, this model gives a linear drop function for the energy drain characteristics.

In order to have a more realistic energy model, a set of experiments was conducted using the Texas Instruments CC2530ZDK nodes. The aim of the experiments was to monitor the energy drain characteristics of the nodes, and plot the drain characteristics for different rates of data traffic. The tests were conducted using two Texas Instruments CC2530ZDK nodes. Implementing a typical point-to-point link, one of the nodes was setup as the collector/gateway, and the other node was setup as a sender, generating UDP (Unit Datagram Protocol) data traffic at a pre-specified rate. For the scope of the study, the

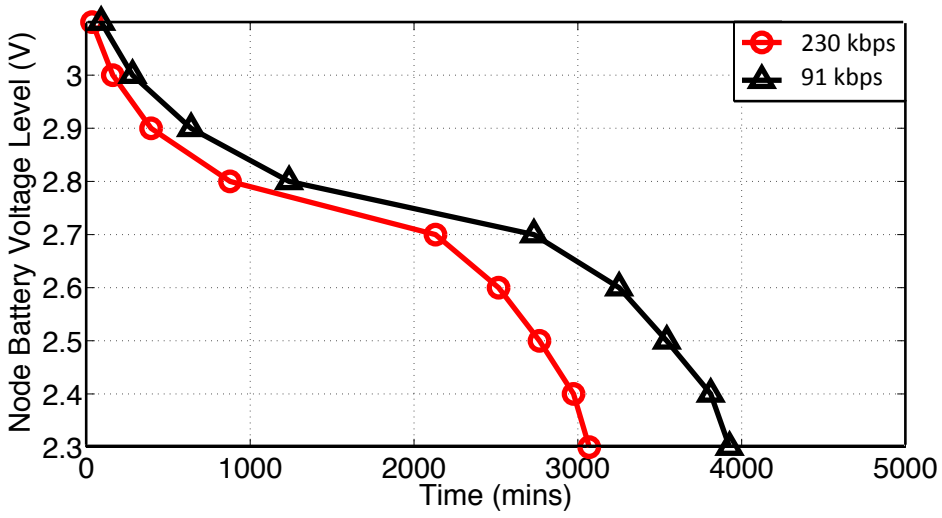

Figure 3.1 Experimental Result Illustrating the Battery Decay Behaviour of TI CC2530 Nodes.

experiments were conducted for 230 kbps, representing 250 packets/second; and 91 kbps, corresponding to 100 packets/second. For both the packet transmission rates, results were computed corresponding to one complete battery discharge cycle. As shown in Figure 3.1, the plot for the residual battery voltage level versus time shows the non-linear battery decay characteristics of the CC2530ZDK nodes. This gives a better insight into the actual battery drain behavior of the kits, as compared to the linear energy drop model given by the default energy model in NS-2. Thus keeping in mind the test-bed battery drain characteristic, the energy model in NS-2 was suitably modified in order to depict the residual energy level of the nodes using the non-linear energy model based on the experimental results computed in this section. To achieve this, the maximum battery level is scaled down so that each node can process the transmission and reception of up to 300,000 packets in order to reduce the time taken to simulate a powered-out node. Thus, based on the number of packets processed by a node, the energy decay of the node is modeled according to the trend shown by Figure 3.1. Hence, this gives a more realistic residual energy level at any given time during the simulation run, which aids in a more realistic and accurate routing behavior.

3.5 Modified Beacon Exchange Mechanism

For effective and efficient routing decisions, one of the major requirements is the availability of updated information regarding the routing parameters. This requirement stands more prominently in case of distributed routing algorithms, as they base their routing decisions on the routing parameters derived from the neighbouring nodes. If the neighbourhood information is not updated regularly, the routing would not function appropriately as it might lead to sub-optimal routing decisions. Thus, it needs to be stated that the control messages, including hello messages or beacon messages hold equal importance as the data packets.

Type	Node ID	Current Location	Residual Node Battery Level	Node Connectivity
1 Byte	**1 Byte**	**2 Bytes**	**1 Byte**	**1 Byte**

Figure 3.2 Modified Beacon Message Packet Format.

The traditional geographic routing algorithm employs a beacon exchange mechanism in which each node broadcasts its updated location along with its node identifier (ID). This type of beaconing procedure is called periodic hello message exchange protocol. In the classical beaconing mechanism, all the nodes receiving this beacon message update this information periodically in their neighbour lists. But, this beacon exchange mechanism suffers from an inherent limitation, as the information exchanged with the neighbour nodes is very limited, and might not be suitable to judge the actual network and node parameters accurately.

In this section, a modified beacon or hello message exchange protocol is proposed. In the system proposed for the TIEGeR algorithm, for each hop, the metric requires additional information regarding the node connectivity, the residual energy level of the node and link quality between the two nodes, along with the current node location and node identity information. So the hello message packet will be prepared accordingly by picking up the required values from the nodes and periodically broadcasting the same to all the neighbouring nodes. In the modified framework for the beacon message exchange protocol used for TIEGeR (see Figure 3.2), all the nodes periodically broadcast a hello packet to all neighbouring nodes within the transmission range. These hello packets contain updated information regarding the node's current geographic location, node residual energy level and node connectivity information in terms of the number of *Forward Progress* neighbouring nodes available, along with the node ID. All the parameters required for the hello message are computed using the models discussed above in the preceding sections. Once this hello packet is received by a node, it updates all the values for the node parameters in the neighbour list entry corresponding to the source of the hello packet. The node consequently uses

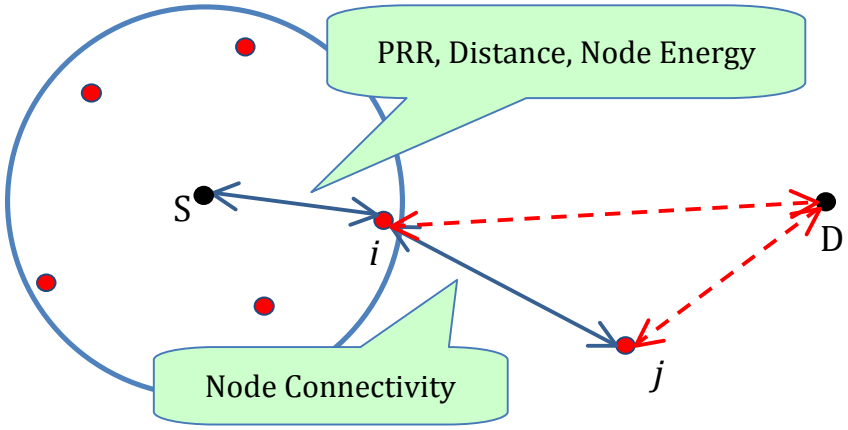

Figure 3.3 Two-Hop Information Considered for Routing Decisions.

these entries whenever it has a data packet to be forwarded towards the destination node.

The *beacon exchange protocol* can be summarized as follows:

a. *Sending hello packets*: All nodes periodically broadcast hello messages containing node ID, node's location, residual energy, connectivity factor.
b. *Receiving hello packets*: On receiving a hello packet from node *j*, node *i* updates its neighbour table with values carried in the received hello packet.

3.6 Proposed Multi-Parameter Routing Metric

Presented in this section is a new routing decision making scheme, which combines the effects of multiple network and node parameters. We utilize node connectivity information, the link quality information between the current and the candidate nodes, the residual energy level of the candidate node along with the distance of the candidate node from the destination node to formulate the routing metric. As shown in Figure 3.3, we use link quality, distance progress towards destination and residual energy level of the candidate node for the first hop, and node connectivity index information for each candidate node as the parameter related to the second hop being investigated for the scope of the routing decision.

Let the current node be denoted by *i* while its candidate neighbour node by *j*. The routing decision is based on the following metric:

$$w_{i,j} = \left[\alpha \,.\, p_{i,j} + \beta \,.\, c_j + \delta \,.\, \overline{E_J}\right] \quad (5)$$

where $(\alpha + \beta + \delta = 1)$.

In the above metric $w_{i,j}$, $p_{i,j}$ refers to the link quality for the link between current node *i* and 1-hop neighbour node *j*. c_j is the node connectivity information for the candidate node *j,* which gives an indication of the number of *forward progress* nodes present in the neighbourhood of the candidate node *j*. In other words, c_j denotes the number of neighbours available to forward the packet successfully towards the destination node. This gives an indication of the second-hop connectivity for the current node *i*. The primary motivation behind using the connectivity factor is to predict the location of the routing void in the network and avoid routing the packet towards a routing void. $\overline{E_J}$ refers to the normalized node residual energy of candidate node *j*. Also, α, β and δ denote the weight parameters for link quality, connectivity and residual energy level, respectively.

The routing decision is based on the maximum value of $w_{i,j}$ among all the candidate nodes *j*. The requirement from the metric is to provide with a next-hop node that has the best link quality factor among all candidate nodes denoting a good Link Quality as compared to the rest of the candidate nodes. At the same time, it is desirable to choose the next-hop from the *forward progress* candidate nodes, indicating a proximity to the destination node D. The intuition behind formulating this metric with the node connectivity information is to avoid sending a packet to a node that might lead to a deadlock situation by routing towards a routing void. The basic principle is that the greater the number of forwarding nodes available, the higher will be the node connectivity and node density, thus avoiding a situation where the packet might be forwarded to a node with no available forward progress node, leading to the routing void. This behavior of the routing metric is exploited by setting the weight associated with the connectivity parameter to a sufficiently large value so that the overall contribution of the connectivity factor in the routing metric weight is clearly visible during routing decisions. Using this metric, it can be seen that it may lead to avoiding the routing

void to a great extent by fore-warning the current node *i* about possible local maxima nodes.

Moreover, in order to avoid nodes with low residual battery levels being overused during routing packets, the node residual energy level term is used to decide among nodes with low residual energy levels and those with higher residual energy levels. For the scope of this algorithm, we give the highest importance to the energy balancing term in the routing metric so as to aid in higher network lifetime. Setting the weighting factor for the node residual energy level slightly higher than the other two weighting factors in the routing metric does this. This leads to effective energy balancing as it avoids routing packets through nodes with low energy levels, thus helping increase the network lifetime by reducing the possibility of node failures. If we encounter a situation where all nodes in the candidate nodes set are low on residual energy level, this routing scheme will still be effective, as it will then choose the node with the highest routing metric value. In that case, the decision will be based on the connectivity factor value as well as the link quality index for the candidate nodes.

3.7 TIEGeR Algorithm

Greedy forwarding is usually the most efficient forwarding strategy among all Geographic Routing Schemes. In this section, we present the proposed TIEGeR algorithm that still follows the idea of geographic routing except using weight $w_{i,j}$ to replace sole geographic distance as a contributing factor towards the routing decision. The weight $w_{i,j}$ is computed using the routing metric discussed in Section 3.7 above. The idea is to bypass the void area as soon as possible and to keep using greedy forwarding in the dense area while forwarding the packet in an energy efficient way in order to achieve effective energy balancing throughout the network, and hence, to increase the network lifetime. The TIEGeR algorithm has the following steps:

1. When node *i* receives a data packet, compute $w_{i,j}$ using (5)

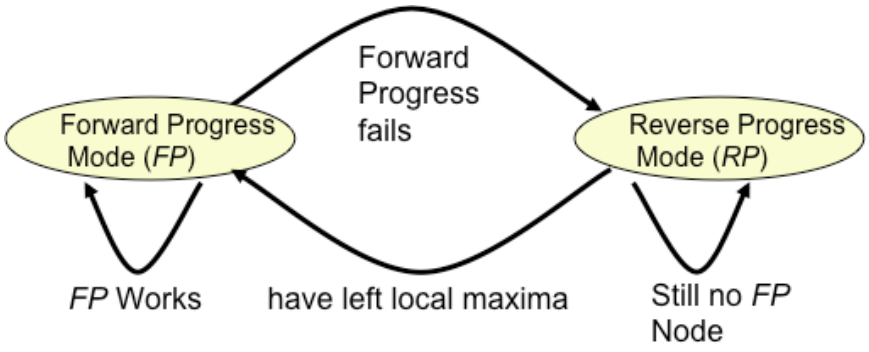

Figure 3.4 TIEGeR Algorithm Routing Mode Flow.

2. ***Forward Progress Mode***: If $\left|N_i^{FP}\right| \geq 1$, choose next-hop j^* such that:

$$j^* = \arg \max_{\forall\, j \in N_i^{FP}} w_{i,j}$$

3. ***Reverse Progress Mode***: If $\left|N_i^{FP}\right| = 0$, choose next-hop j^* such that:

$$j^* = \arg \max_{\forall\, j \in N_i^{RP}} w_{i,j}$$

TIEGeR algorithm uses 2-hop neighbour information to compute the routing metric. The motivation behind using different parameters for the two hops under consideration is to reduce the overhead due to calculation of the metric over the second hop. As we only consider the node connectivity factor over the second hop, this reduces the overall computation time and energy utilized for such computations over each metric run computation cycle. The first hop computation is more computationally intense as this is the link the packet will be traversing.

Even though TIEGeR reduces the possibility of encountering a routing void due to the additional information regarding the node connectivity status helping predict the nodes close to routing voids, there still might exist some situations leading to routing voids. Under such circumstances, the algorithm switches over to reverse progress mode, wherein the current node routes the packet to the reverse progress node returning the maximum value of the weight $w_{i,j.}$ among all available reverse progress candidate nodes. This behavior, as depicted in Figure 3.4, is continued till the packet reaches a node where forward progress greedy forwarding can be re-applied. Consequently, the algorithm is able to retain the

advantages of multi-parameter greedy forwarding even in the deadlock situations when a packet encounters a routing void during its progress towards the destination node. Furthermore, this helps alleviate the inherent limitations of the secondary routing scheme in geographic routing algorithms, i.e., the perimeter forwarding scheme, which lacks the ability to forward packet considering node residual energy and the link quality of the link being chosen for the next-hop. This essentially means that even in special conditions where a packet is stuck in a routing void, the packet will still be forwarded in an energy efficient multi-parameter greedy method, by employing the modified routing metric presented here. The pseudo-code implementation of the TIEGeR algorithm is shown in Algorithm 3.1.

ALGORITHM 3.1: TIEGeR Algorithm

Variables: current node i, destination d, received packet P, Neighbour Set N Forward Progress Neighbour Set N^{FP}, Reverse Progress Neighbour Set N^{RP}

BEACON-UPDATE*(P)*
{
if *P.Type* == beacon packet type
    if *P.Source* exists in neighbour set N_i of node i
        update node location, connectivity, residual battery level
        for *P.Source*
    endif
    else if *P.Source* does not exist in neighbour set N_i of node i
        create new entry in N_i
        store current location, connectivity, residual energy level
        for *P.Source*
    endif
endif
}

TIEGeR*(P)*
{

if *P.Type* == data packet type
    if current node *i* == destintion node *d*
        packet reception successful
        log packet information
        return
    endif
    else
        compute distance from destination d_i
        for each entry *j* in neighbour list N_i
            calculate distance d_j
            calculate link quality $p_{i,j}$
            calculate connectivity c_j
            get residual energy level $\overline{E_j}$

            Using the above values, compute routing weight $w_{i,j}$
            If $d_j \leq d_i$
                Routing Mode = Forward Progress Mode
                next-hop $j^* = \arg\max_{\forall\, j \in N_i^{FP}} w_{i,j}$
                return
            endif

            else
                Routing Mode = Reverse Progress Mode
                next-hop $j^* = \arg\max_{\forall\, j \in N_i^{RP}} w_{i,j}$
                return
            endif
        endfor
    endif
}

3.8 Implementation of TIEGeR in an IEEE 802.15.4 Environment

We implement the proposed TIEGeR Algorithm in an IEEE 802.15.4 environment using both simulation based on NS-2 [35] and experimental testbed

based on TI CC2530ZDK. For simulation, the code is developed using the GPSR implementation by Ke Liu [40]. To implement the proposed TIEGeR algorithm, the GPSR code was modified with the added modules related to the modified beacon mechanism along with other additions/changes required for the four routing factors being considered to compute the modified routing metric as discussed in Section 3.6. TIEGeR is compared to existing geographic routing schemes like GPSR, GRR, PRR*D and GEAR by simulating different network topologies using NS-2. The IEEE 802.15.4 MAC layer implementation by [39] is used. Even though TIEGeR is a generic routing algorithm that can function on any MAC and PHY layer architecture, the 802.15.4 MAC and PHY sublayers are used essentially to keep the simulation results in line with the experimental results using the TI CC2530ZDK based test-bed. As the CC2530 nodes use the IEEE 802.15.4 standard as their inherent MAC and PHY layers, the parameters for the NS-2 MAC layer have been modeled carefully to replicate the testbed MAC layer. These CC2530 nodes provide an ideal testbed to investigate any routing algorithm, as they provide the flexibility to develop custom-made routing algorithms over the 802.15.4 standard specific PHY and MAC layers. The composition of the protocol stack for TIEGeR is illustrated in Figure 3.5.

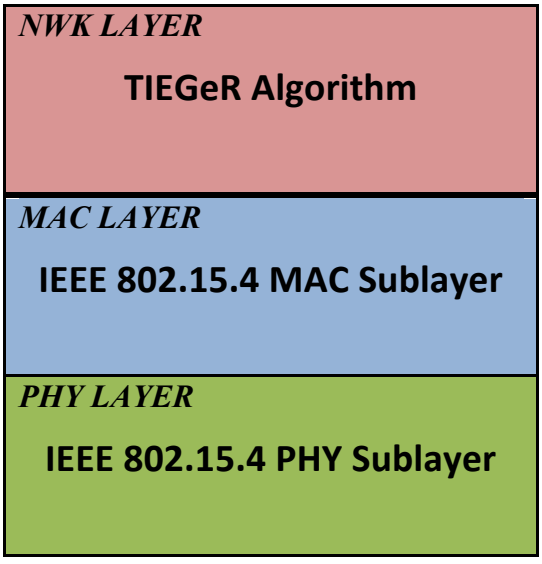

Figure 3.5 Protocol Stack Structure for TIEGeR.

For the simulation scenarios, each node is set to have a maximum transmission range of 40 meters. The weight parameters α, β and δ for the routing metric $w_{i,j}$ are set as 0.3, 0.3 and 0.4, respectively, laying maximum importance onto the residual energy parameter. The path loss exponent γ and the shadowing deviation X_{dB} for the link quality model is set as 3 and 4 dB, respectively. In order to have a realistic energy model for the simulations, we use the energy level decay function based on the experimental testbed measurement results based energy model discussed in Section 3.4. This way, the linear default battery model of NS-2 is updated to a more realistic non-linear energy model inherited from the testbed. General parameters relevant for both experimental testbed and simulation platform are described here. These parameters are for non-beacon enabled mode, using unslotted CSMA-CA channel access mechanism.

- *Traffic Type*: We generate a Constant Bit Rate (CBR) application traffic based on the UDP (User Datagram Protocol). Its primary features are Single Way Transmission (No Acknowledgements), Defined Packet size and Defined Packet Interval. File Transfer Protocol (FTP) traffic with a Transmit Control Protocol (TCP) connection is also possible. However, due to its features like congestion control, requiring dynamic adjustment of the transmission rate based on the traffic conditions, delivery ratio would be 100%. Hence, performance metrics like packet delivery ratio would be meaningless in such cases as the network could not be tested for the effect of congestion.
- *Packet Size*: The data payload size in a data packet is fixed as 114 bytes. This is exclusive of the MAC and PHY layer headers. The total packet size, inclusive of all headers and footers is 127 bytes. The packet format for the packets being transferred in TIEGeR, including the NWK (Network), MAC and PHY layer headers, is illustrated in Figure 3.6. It illustrates the hierarchical breakdown of the packet fields, starting from the Network layer packet structure for a typical Beacon Message and Data Packet. The MAC sublayer packet, complete with the MAC Header (MHR) and the MAC Service Data Unit (MSDU), follows this. This MAC layer

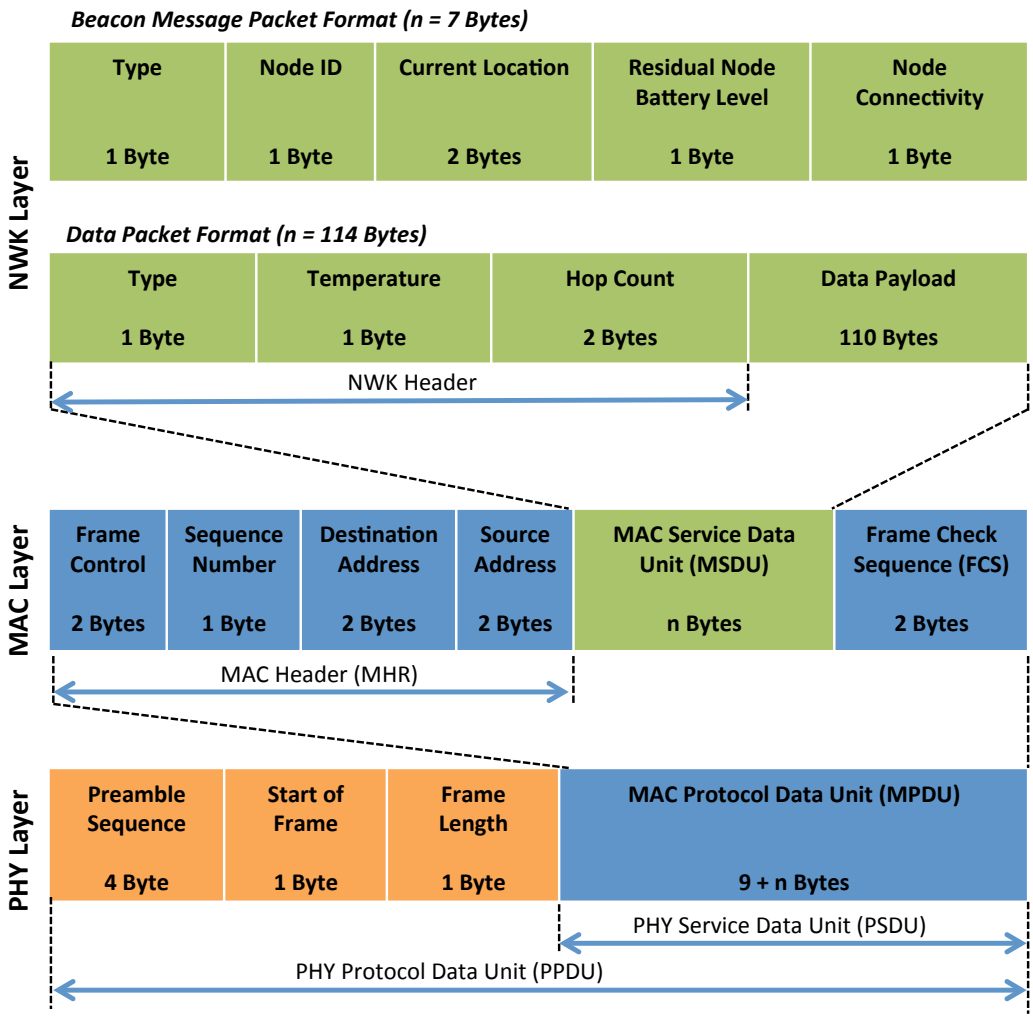

Figure 3.6 TIEGeR Packet Formats.

packet is further encapsulated into the PHY Service Data Unit (PSDU) of the PHY layer. Finally, this PHY layer packet, with the PHY headers is transmitted over the air using the radio transceivers.

- *Traffic Direction*: The data traffic is unidirectional, with the transmission directed towards the coordinator/gateway node.

Before delving into the large-scale simulations emulating the real time effects for the TIEGeR algorithm, we present a few test cases, which were implemented for a thorough operational verification of the various steps and modes of the TIEGeR. These test cases are discussed in Subsection 3.9 in more details.

3.9 Operational Verification of the TIEGeR Algorithm

In order to examine, verify and correct the behavior of the TIEGeR algorithm, a few simple network topologies are simulated with the two routing algorithms being compared, TIEGeR and GPSR. The aim is to check the efficacy of the presented algorithm in terms of the improvements over the traditional GPSR routing algorithm. This includes a critical case, wherein the source node is deliberately placed in close proximity of a routing void, with no forward progress nodes available. The main idea behind this topology is to simulate and verify if the *reverse progress* mode of the TIEGeR routing algorithm functions as expected, and is able to circumnavigate around the routing void in energy efficient and link quality aware fashion. A brief discussion about each of the test cases and the primary goal behind them is presented in the proceeding subsection.

3.9.1 Test Setup 1

In this test setup, we simulate a network of 11 nodes as shown in Figure 3.7. The source and the destination nodes are placed on the two opposite ends of a 9 node square grid with nodes placed equidistantly at a distance of 4 meters from each other both on *x* as well as *y* axis. The source node generates CBR traffic at a rate of 9 kbps, equivalent to 10 PPS (Packets Per Second). The CBR traffic is generated for duration of 150 seconds per simulation run of 250 seconds. This allows ample amount of time for the simulation to initialize all the relevant

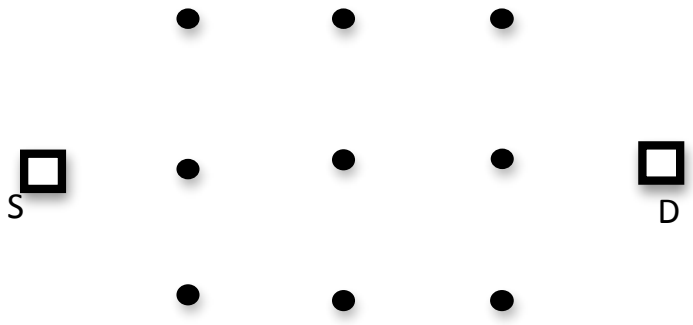

Figure 3.7 Test Setup 1.

network and node parameters. Also, with a suitable duration of time between the end of data packet flow and end of simulation, the simulation platform is able to compute and compile the results effectively. The primary objective of this network topology is to verify the energy balancing behavior of the proposed routing scheme. This is done by first analytically solving for the presented network topology and determining the weight $w_{i,j}$ for all the candidate nodes in the current node's neighbourhood. This is done for a series of iterations and, for each iteration, the residual energy of the nodes being utilized for the last packet transferred is updated with the new residual energy level. Thus, after a sufficiently large time interval, the packets being transferred between the source and the destination node exhibit a change in the path taken for packet traversal. Simulating the network topology for test case 1 and examining the resulting NS-2 trace file for the path taken by the subsequent packets in the network over the duration of data packet transmission in the network verified this behavior.

It was observed that the packets indeed took many alternate paths during the entire 150 seconds duration of data transmission. This was due to the residual node energy parameter of the static network topology varying over time, thus returning a different value each time a packet arrives at a node in the network to be forwarded towards the destination. Table 3.1 shows the simulation results for both GPSR and TIEGeR. On comparing the simulation results with those for the traditional GPSR routing algorithm, it was interesting to notice that due to the energy balancing property of the proposed routing scheme, the proposed TIEGeR algorithm outperformed GPSR in terms of both the Packet Delivery Ratio as well as the Network Lifetime of the test network. This can clearly be attributed to the fact that GPSR tends to use the same path towards the destination node repeatedly,

Table 3.1: Simulation Results for Test Setup 1

	TIEGeR	**GPSR**
Packet Delivery Ratio	113/150	76/150
Network Lifetime (seconds)	185	140

without considering residual energy levels of the nodes being utilized. This leads to the nodes depleting their limited energy reserves much faster as compared to the TIEGeR algorithm. Moreover, as the nodes along the shortest path being utilized by GPSR power out, it leads to packets being dropped for a brief interval before the timeout for the entry in the neighbour list of the other neighbouring nodes occurs. Clearly, as energy is actively included into the routing decision for the modified routing metric utilized by TIEGeR, the packet loss due to energy depletion of the nodes is relatively much smaller as compared to that for GPSR.

3.9.2 Test Setup 2

This test setup corresponds to a special case to test the performance of the proposed routing algorithm while running in the *reverse progress* mode, i.e., when no candidate node is available in the *forward progress* direction. The key inspiration of this test scenario is to verify the behavior of the routing algorithms being compared in case of encountering a routing void.

For the scope of this test case, we simulate a network topology consisting of a topology of static nodes along with a routing void placed deliberately between a pair of source and destination node. The architecture of the topology along with the node placements is shown in Figure 3.8. This is done so that a direct forward progress path to the destination node from the source node is unavailable, thus forcing GPSR to switch over to secondary forwarding scheme, the perimeter

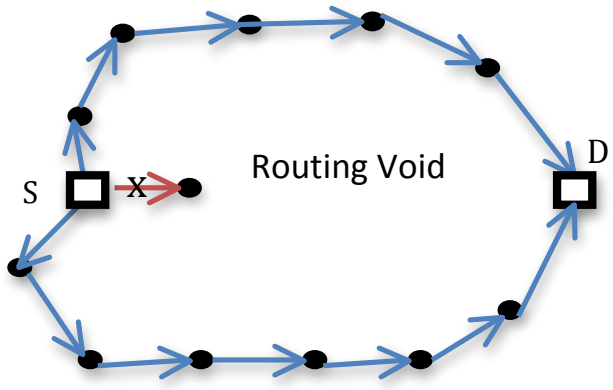

Figure 3.8 Test Setup 2.

routing algorithm. This will enable a fair comparison of the two routing algorithms being compared, especially in deadlock scenarios. Also, in order to verify the energy balancing capability of the TIEGeR in the *reverse progress* mode, there are two independent paths simulated towards the destination node, as shown in the Figure 3.8.

The objective behind this is to examine if the two available paths are adequately utilized throughout the simulation run to cater to the energy levels of the *negative progress* nodes for source node S. As GPSR lacks the capability to forward packet in an energy efficient manner while running in the secondary routing scheme, it will intuitively end up utilizing the same path over the entire duration of the simulated packet flow, thus exhausting the energy reserves of the nodes along the path being recurrently used leading to nodes powering out earlier as compared to TIEGeR. To verify these intuitive claims regarding the proposed TIEGeR algorithm, we simulate CBR traffic from source node S towards the destination node D for duration of 150 seconds out of the entire 250 seconds simulation runtime. On close analysis of the trace files for both the routing algorithms, it was noted that the proposed routing scheme was indeed able to juggle between the 2 available paths as marked in Figure 3.8 above, effectively causing energy balancing between the two available paths towards the destination node. On the contrary, GPSR tends to forward the packet to the deadlock node as marked by the X arrow in the Figure 3.8. At this stage, the perimeter routing mode of GPSR is initiated, which tends to use a single path towards the destination node for all the packets being transmitted though the network. This leads to the nodes along that path to die out much earlier, consequently having a much smaller network lifetime as compared to the network lifetime of the proposed routing algorithm. The behavior discussed in this test case matches the expected behavior of the proposed routing algorithm as well as GPSR.

Chapter 4

TIEGeR: Performance Evaluation

This chapter presents a comprehensive performance evaluation of the proposed TIEGeR algorithm using both simulation and experimental results. By simulation, we investigate the performance of the proposed TIEGeR algorithm in large-scale network topologies. By experiment, we further evaluate and demonstrate the operation and performance advantages of the TIEGeR scheme implemented in the network layer of a WSN using the IEEE 802.15.4 MAC/PHY layers. Section 4.1 discusses the performance parameters/metrics used for evaluation. Section 4.2 presents the performance evaluation of the IEEE 802.15.4 PHY/MAC layers to identify their performance limitations and characteristics, which are used as reference for the subsequent performance evaluation of the routing algorithms. Both experiment and simulation are used to examine the effects of the data rate, propagation losses with increasing distance between the two nodes in a typical point-to-point link, and the effect of multiple source nodes transmitting simultaneously emulating a typical multipoint-to-point environment. In Section 4.3, a comparative study of the proposed TIEGeR algorithm with comparable geographic routing schemes is conducted. This comparative evaluation combines the simulation and experimental results highlighting the advantages of using node residual energy level, node forward connectivity and link quality estimates in various network scenarios.

4.1 Evaluation Parameters

In order to effectively compare the performance of the proposed TIEGeR algorithm with the pre-existing Geographic Routing schemes, we use the following performance metrics:

- **Packet Delivery Ratio** (PDR)**:** This is defined as the ratio of number of packets successfully delivered at the destination node to the total number of packets generated at the source node.

- **Network Lifetime:** This is the time before the first node in the network dies out due to depletion of its energy resources. The objective is to measure the time before the network partitions due to energy depleted node.

The first metric is used to measure the packet reception success probability on the network using the routing algorithms being compared. This will show us how using the additional information regarding the link quality estimates on the path of a packet can aid in improving the overall packet delivery ratio. By choosing the paths with higher link quality as compared to the traditional geographical routing algorithms that do not consider the effect of link quality for any links on the path of a packet, the overall packet delivery ratio of the TIEGeR is considerably higher.

The second metric is related to the effective energy balancing capability of the TIEGeR algorithm. Here, the network lifetime relates to the maximum amount of time before any of the nodes in the network powers out due to depletion of the limited energy resources of that node. As one of the objectives of the proposed routing scheme is to maximize the lifetime of the network, in effect, the TIEGeR algorithm functions to increase the time interval between the start up of the network and the time when the first node in the network powers out. The assumption being made here is that any node powering out due to depletion of the energy resources can lead the overall network topology being disrupted, which might lead to partitioning of the network for certain bottleneck nodes in the network. It is interesting to see how well TIEGeR adapts to situation where nodes with critical energy levels are avoided for further transmission of packets. This is a primary performance characterization of TIEGeR where energy balancing is a critical milestone for performance enhancement.

4.2 Performance of IEEE 802.15.4 MAC/PHY Layers

As the performance evaluation will be conducted with the routing algorithms implemented on top of the IEEE 802.15.4 MAC/PHY layers, it is important to identify the limitations posed by the 802.15.4 functionalities as the reference. For this, we will first evaluate and characterize the performance of the IEEE 802.15.4 MAC/PHY layers by simulations and experiments. These results will then be used as reference in the subsequent performance evaluation of the network layer that uses the proposed TIEGeR or different other geographical routing schemes for comparison (to be presented in Section 4.3).

In the following, we will examine the effects of the rate of data traffic generation, propagation losses with increasing distance between the two nodes in a typical point-to-point link, and the effect of multiple source nodes transmitting simultaneously emulating a typical multipoint-to-point environment.

4.2.1 Point-to-Point Free-Space Transmission Performance

The first set of experiments was conducted to evaluate the effects of increasing transmission rate on the packet delivery ratio performance over a point-to-point free-spaces link. Experiments were set up in an anechoic chamber to represent an ideal free-space propagation environment. The IEEE 802.15.4 standard advertises a maximum transmission data rate of 250 kbps (See Appendix A). However, due to several overheads induced by the typical messaging protocols implemented, the achievable maximum throughput has been investigated in [36-39] to be lower than the upper bound of 250 kbps. Taking into consideration all the MAC and PHY layer overheads, [36] estimated a maximum achievable data throughput of around 153 kbps. Our first set of experiments aims to verify and evaluate this achievable maximum throughput. A point-to-point link using 2 CC2530ZDK nodes is set up in an anechoic chamber, with one of the nodes initialized as the coordinator/gateway and the other node setup as the end device. The direction of the data traffic is fixed from the end device towards the coordinator. In order to have a steady flow of traffic towards the coordinator, the end device generates

CBR (constant bit rate) data packets and forwards them to the coordinator node. As the experiments are being conducted inside the anechoic chamber, the propagation model can be considered as the free space model and the effects of collisions with other packets in the surrounding environment as well as the effects of multipath can be safely and reliably eliminated. Hence, the only losses that occur in these tests are the losses due to the PHY and MAC sublayer limitations. This will be instrumental in forming the reference for the performance evaluation of the routing algorithms later on by segregating the limitations due to the MAC and PHY sublayers.

In order to study the effect of increasing distance between the 2 nodes in the test-topology, for a pre-specified packet generation rate, the distance is varied from 0 to 5 meters. The same test is repeated for various packet generation rates: 10, 50, 100, 150, 200 and 250 packets per second (PPS), which are roughly corresponding to throughputs of 9, 45, 90, 135, 180 and 240 kbps, respectively.

Figure 4.1 shows the plots of the measured Packet Delivery Ratio (PDR) versus the distance between the end device (sending node) and the coordinator/gateway (receiving node). As expected, the packet delivery ratio for the data packet rate up to 150 PPS is 100% for all the distances from 0 to 5 meters. This is in agreement

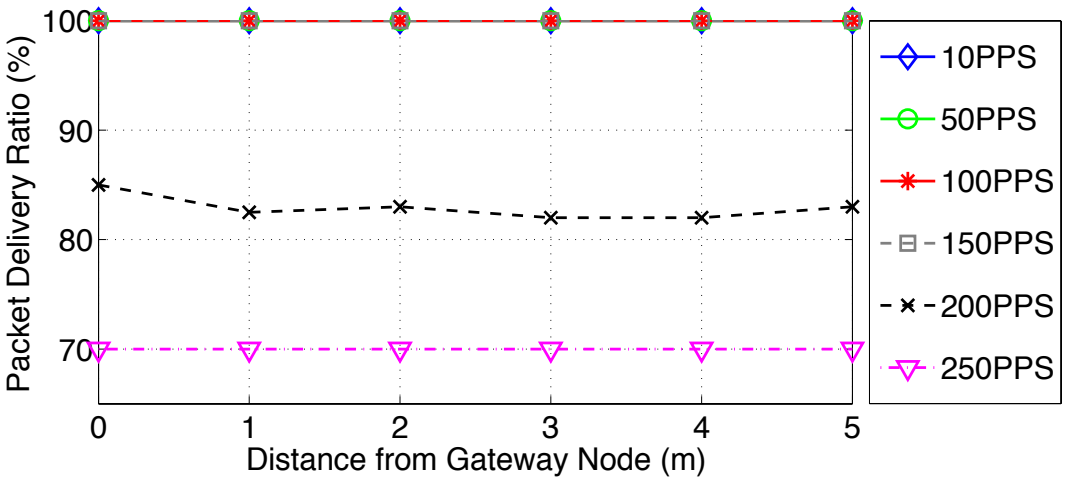

Figure 4.1 Packet Delivery Ratio versus Node Distance from Gateway (Free Space Propagation Model).

with the maximum achievable throughput of 153 kbps estimated in [36]. As the data packet rate increases beyond 150PPS, the 802.15.4 PHY/MAC layers induced limitations as indicated in Figure 4.1: The plot shows a considerable drop in the PDR for the 200 PPS case. On an average, nearly 19% of the total packets generated by the sender end device are lost at the destination gateway node. For the case of 250 PPS (230 kbps), the drop in the overall packet delivery ratio is even higher. The average packet delivery ratio for 250 PPS over all the distance profiles is 70%.

4.2.2 Point-to-Point Transmission Performance

The second test scenario also deals with a point-to-point link between two nodes but in a realistic non-free-space propagation environment. The point-to-point link setup is the same as the one used in Section 4.2.1: One of the nodes is setup as a typical coordinator/gateway node, while the other node is setup as an end device, generating CBR data traffic towards the coordinator. We conducted the performance evaluation using both simulation and experiment. In simulation, a shadowing propagation model is used while the experiment is set up in a typical indoor office environment. The transmit power level is padded down using sufficient level of attenuation so that the effective range of the transmission is limited to a maximum of 10 meters.

Simulation results are presented in Figure 4.2. Clearly, the packet delivery rate decreases as the distance between the end device and the gateway node increases. The measured PDR depicts a drop with increasing traffic load. Similar characteristics are also observed in the experimental results plotted in Figure 4.3. Even though for both the experimental and simulation results, all the test cases up to 150 PPS show a similar PDR of around 98 % for the 2 nodes placed adjacent to each other, the simulation platform results return a slightly higher value for PDR as compared to the corresponding experimental result. This could be attributed to the fact that the propagation model in the simulation platform is based on the shadowing model, and ignores the effects of fast fading. Moreover, as seen in Figures 4.2 and 4.3, the PDR for the higher traffic generation rates of 200 and 250

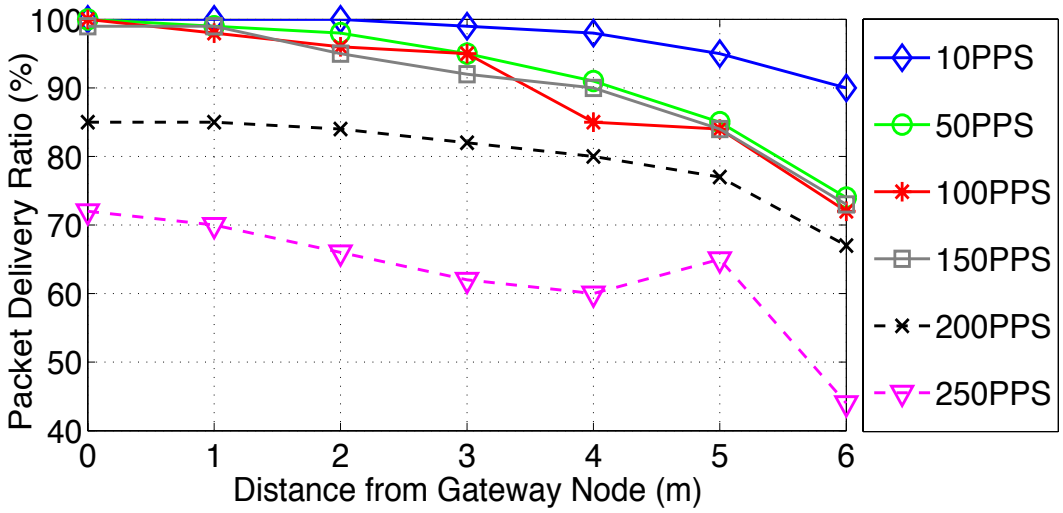

Figure 4.2 Packet Delivery Ratio versus Distance of a Point-to-Point Link in a Shadowing Propagation Environment (Simulation Result).

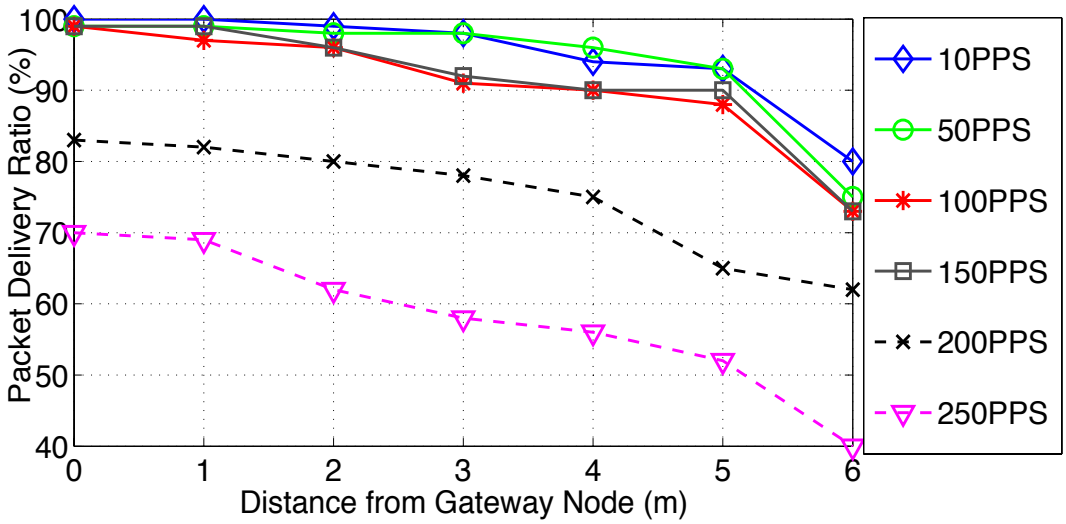

Figure 4.3 Packet Delivery Ratio versus Distance of a Point-to-Point Link in an Indoor Environment (Experimental Result).

PPS show a considerably lower value as compared to the PDR for rates up to 150 PPS. As discussed in the previous test case, this drop in the PDR is due to the 802.15.4 MAC/PHY layers induced limitations. Furthermore, for the cases where the two nodes are adjacent to each other (Figure 4.2 and 4.3), the PDR is the same

as reported for the free space model in Figure 4.1. This means that for the closely spaced nodes, the loss of packets is primarily due to the 802.15.4 MAC and PHY layers limitations, and not the environmental factors like propagation loss, multipath, collisions or interference from other wireless devices working in the same frequency band. As the distance between the two nodes increases, the rate of drop in PDR increases. Clearly from Figure 4.2 and 4.3, the worst performance is displayed by 250 PPS case, whose PDR drops down to around 40 % for the distance of 6 meters between the two nodes.

4.2.3 Transmission Performance of Multipoint-to-Point Systems

This scenario emulates a typical WSN setting with multiple end devices transmitting CBR data traffic towards a common coordinator/gateway node in a non-free-space propagation environment. The set of experiments follow a trend similar to the set of experiments conducted for test scenario 2, including the simulation and experimental model setup for a non-free-space propagation environment. Initially, the multiple source nodes are placed adjacent to the gateway node in order to minimize the effect of the environmental factors especially the propagation loss. Subsequently, the distance between the set of end devices and the gateway node is increased in steps of 1 meter, up to a maximum distance of 6 meters between the group of end devices and the gateway node. Furthermore, increasing the number of source nodes starting from 1 source and increasing to 3 and 5 Source nodes analyze the effect of multiple traffics towards the gateway node. The same experiment is repeated for three traffic generation rate profiles: 10 PPS, 50 PPS and 100 PPS. Figures 4.4 and 4.5 show the packet delivery ratio versus the increasing distance separation between the group of active source nodes/end devices and the gateway node for the simulation and experimental setup, respectively. One important observation that can be deduced from simulation and experimental results presented in Figures 4.4 and 4.5 is that for low rate traffic generation profile, the packet delivery ratio is unaffected by the addition of multiple source nodes. Comparing the multipoint-to-point results in Figures 4.4 and 4.5 for 10 PPS with higher traffic rate profiles show that the

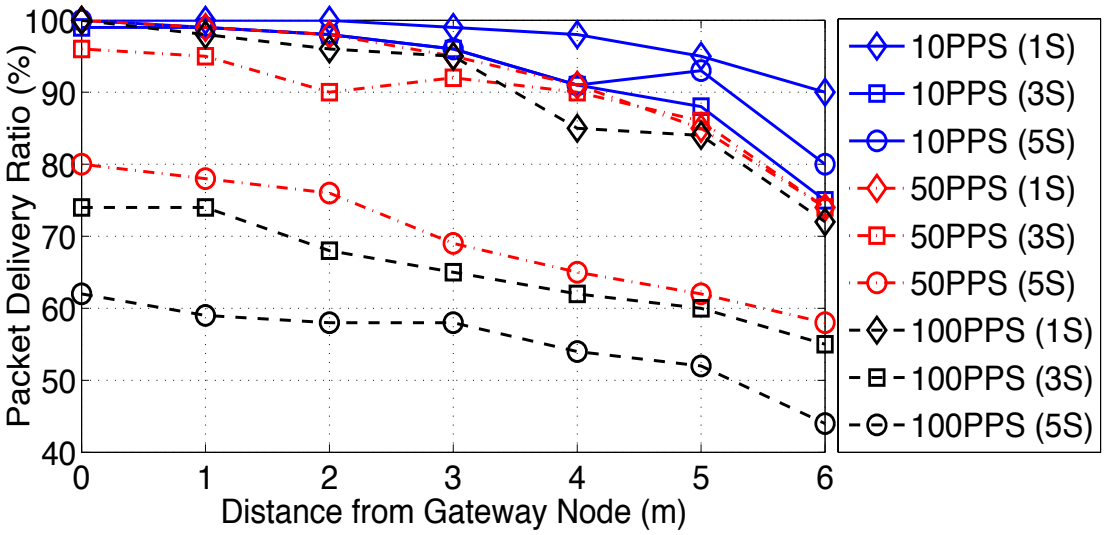

Figure 4.4 Packet Delivery Ratio versus Node Distance from Gateway (Test Scenario 3 Simulation Result).

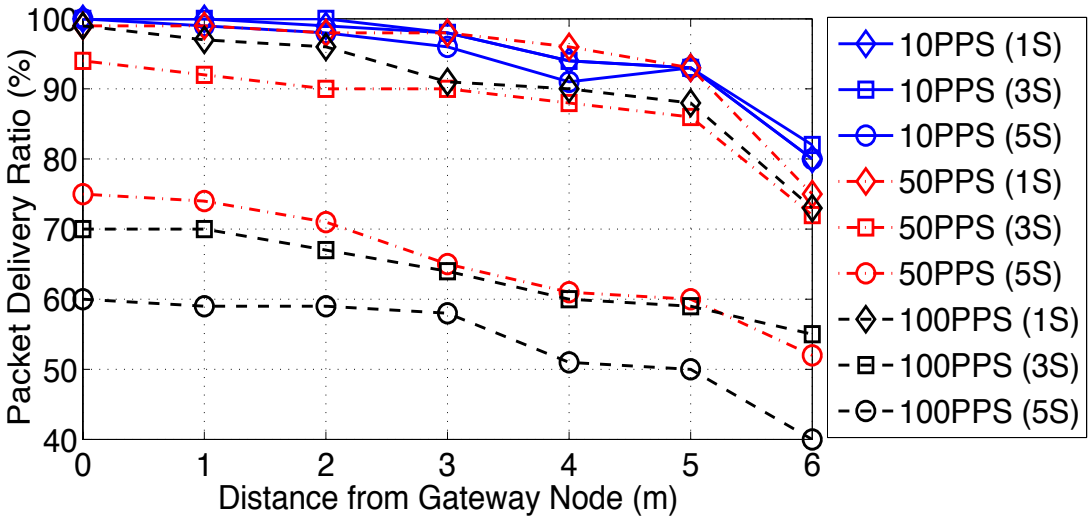

Figure 4.5 Packet Delivery Ratio versus Node Distance from Gateway (Test Scenario 3 Experimental Result).

packet delivery ratio measured for all the three profiles (1 Source, 3 Sources and 5 Sources) is approximately the same, hovering above 95% mark for distance up to 5 meters between the set of source nodes and the gateway node. The losses occurring at these low rates are primarily due to the propagation losses. As the

data generation rate is low, the nodes have enough time to compensate for the delays induced due to packet collisions or the random backoff delays caused by the unslotted CSMA-CA mechanism. On the contrary, looking at the plot of PDR for 50 PPS at different distance separations, the difference between the results for 3 sources and 5 sources transmitting towards the gateway shows a prominent drop. As seen in both experimental and simulation results, when the *total* traffic received at the gateway node crosses the 153 kbps threshold, the packets encounter a steep drop in the PDR. This drop is further increased with increase in the distance between the set of active sources and the receiving gateway node. When the total traffic received at the gateway node is less than 153 kbps, as is the case with 3 active sources generating data packets at 50 PPS, the PDR is around 90%. For the traffic rate of 100 PPS and 3 active sources, the packet transmission suffers from extensive losses due to both the propagation environment and the 802.15.4 MAC/PHY layer limitations. These losses are further compounded with increased number of active source nodes and separation between the set of active source nodes and the gateway node.

4.3 Performance of Routing Schemes

To measure the improvements presented by TIEGeR over the traditional geographic routing algorithms, all the comparable geographic routing schemes are compared using extensive simulations and experimental analysis using the Wireless Sensor Network Testbed comprising of the TI CC2530ZDK sensor nodes. Three network scenarios are considered, each highlighting the importance of the additional information regarding the node residual energy level, forward connectivity and link quality.

Simulation is used to assess the performance of the TIEGeR algorithm for large-scale network topologies, with variable node densities, network architectures and load generation rates. Also, it is beneficial in investigating the network topologies that cannot be tested using the experimental testbed setup. This in turn helps

overcome the limitations of space, mobility and quantity of nodes in the network that is posed by the experimental testbed. All the simulation based topologies in this section follow the simulation environment characteristics as mentioned under Section 3.8. TIEGeR is compared with GPSR and another simulated specialized geographic routing scheme specific to each of the three routing parameters being highlighted. For node residual energy information based analysis, TIEGeR is compared with GPSR and GEAR. GEAR being a popular energy-aware geographic routing scheme, by choosing GEAR, TIEGeR is evaluated against the traditional GPSR and an energy-aware algorithm to illustrate the superior performance of TIEGeR in terms of energy efficient routing capability. Similarly, to illustrate advantages due to forward connectivity information, TIEGeR is evaluated against GPSR and GRR in a typical void scenario. GRR being connectivity aware has been shown to be capable of predicting and avoiding the routing void. Thus, by comparing TIEGeR with the GPSR and GRR, the behavior of the routing algorithms in typical void scenarios is illustrated. For the link quality information based analysis, TIEGeR is simulated with GPSR and PRR*D. As PRR*D considers node link quality in its routing decisions, TIEGeR's performance is evaluated against non link-quality aware GPSR and link-quality information aware PRR*D.

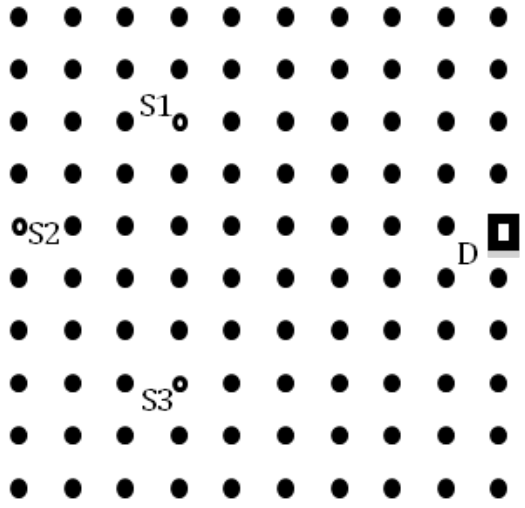

Figure 4.6 Network Scenario 1: Simulation Model (All static nodes, multiple source nodes).

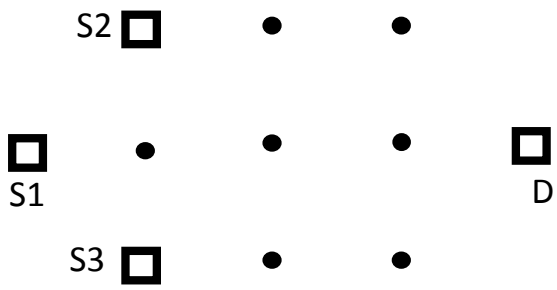

Figure 4.7 Network Scenario 1: Experimental Setup (Multiple source nodes, Variable traffic rates).

Each simulation network topology is complemented with a corresponding experimental testbed topology in order to test the improvements of TIEGeR over the traditional GPSR in the real-life environment. This is done basically to have a comparative analysis between the experimental testbed and the simulation platform.

4.3.1 Improvement due to Node Residual Energy Level Information

We first investigate the goodness of the proposed TIEGeR algorithm in distributing the traffic in the network for achieving efficient energy balancing throughout the network. To test and verify this behavior, we consider a square network topology (Network Scenario 1), for simulation shown in Figure 4.6. Due to area and hardware limitations, the corresponding experimental setup shown in Figure 4.7 has the same configuration of Figure 4.6 but with a reduced area and 11 WSN nodes.

We start with one Source-Destination pair, as shown by source node S1 and destination node D in Figure 4.6 and 4.7. The number of active source nodes is increased from 1 to 3, as depicted by nodes S1, S2, and S3 representing source node 1, 2 and 3, respectively. The destination node is the same for all the three traffic sources, thus effectively simulating a typical WSN environment, where the wireless sensor nodes send periodic updates to the gateway node (Destination node D). The idea is to strain the network with increased traffic load density into the network, and then monitor the effect of this increased load on the network

lifetime. In the simulation model, we increase the load in the network by gradually increasing the rate of CBR data packets generation for each active source node from 9 kbps to 230 kbps. One important point to mention here is that even though the load on the network is being increased, the placement of the nodes, and hence the overall architecture of the network, remains static throughout the simulation. To evaluate the effect of increasing load onto the overall network lifetime, TIEGeR is compared with GPSR and GEAR. The reason for choosing GEAR is to compare TIEGeR with an energy-aware routing scheme

Table 4.1 Network Lifetime for Increasing Load

Traffic Pattern	**Network Lifetime (seconds)**		
	GPSR	***GEAR***	***TIEGeR***
One 9 kbps Source	9302	9600	10260
Two 9 kbps Sources	9028	9385	10115
Three 9 kbps Sources	8755	9156	9980
One 45 kbps Source	3464	3690	3917
Two 45 kbps Sources	3322	3595	3842
Three 45 kbps Sources	3187	3519	3767
One 91 kbps Source	1198	1240	1384
Two 91 kbps Sources	1126	1181	1349
Three 91 kbps Sources	1061	1119	1321
One 230 kbps Source	605	620	670
Two 230 kbps Sources	572	595	648
Three 230 kbps Sources	538	580	632

to analyse and quantify the advantage of TIEGeR in terms of energy-efficiency.

Noticeably, from Table 4.1, as the Traffic generation rate is reduced from 230 kbps to 9 kbps, the Network lifetime of TIEGeR shows substantial improvement as compared to both GPSR and GEAR. In GPSR, the drop in network lifetime is much steeper as compared to the drop for the TIEGeR and GEAR algorithms. It can be seen from Table 4.1 that even though the traffic load is increased in the network, TIEGeR still outperforms both GPSR and GEAR, which degrades drastically in terms of Network Lifetime with additional load, both due toadditional sources as well as increased traffic flow rate. Efficient energy balancing effects and use of multiple paths towards the destination by TIEGeR mitigate the effect of additional load. Hence, the effect onto the network lifetime is not as severe as compared to the effect of increased load on GPSR algorithm. GPSR uses the same static path through the network towards the destination node, hence leading to a much faster energy depletion of the nodes along the path. This depletion of energy is accelerated with increasing rate of packet generation for a fixed source destination pair. Moreover, with additional source nodes added in the network, the flows for the additional traffic being generated might create a bottleneck situation around the nodes close to the destination node. This worsens the network lifetime, as the traffic generation rate of all the active traffic sources increases. Similarly, GEAR also tends to forward the packets in a distance based greedy fashion, not considering the energy efficiency parameters until the pure greedy forwarding fails to navigate towards the destination. At this point, GEAR initializes its estimated-cost function, which is a weighted sum of distance and residual energy level. In the simulation model for Network Scenario 1, the layout is such that both GEAR and GPSR are able to find distance based greedy forwarding paths towards the destination. What this implies is that due to the high density of nodes in the network and the placement of the source nodes, the source nodes are always able to forward the packet in a greedy fashion, which corresponds to the forward-progress mode of the TIEGeR. Thus, both GEAR and GPSR tend to utilize the same path repeatedly until the nodes on this path power-out.

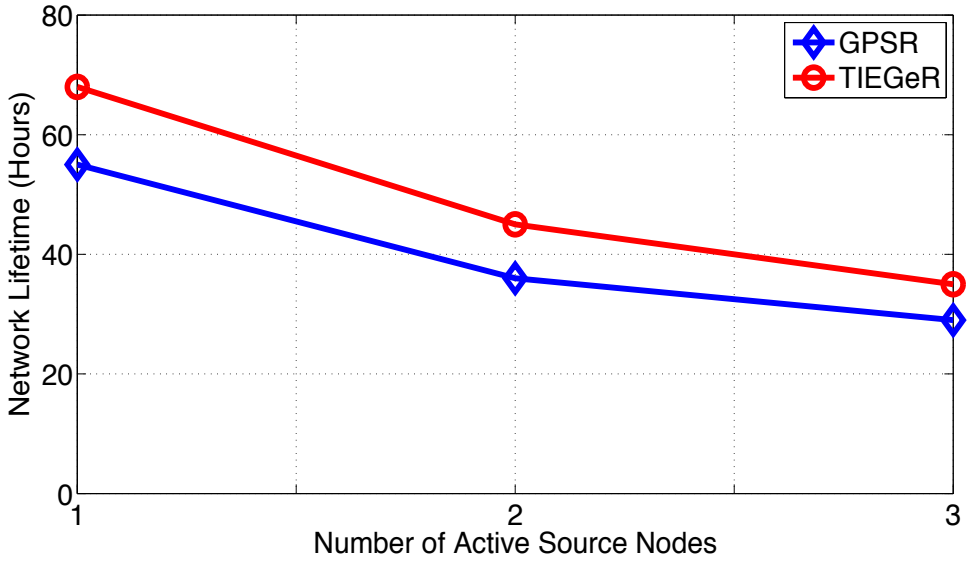

Figure 4.8 Network Lifetime versus Number of Active Source Nodes: Experimental Results (250 PPS).

For the experimental setup (Figure 4.7), the measured results show a similar trend as the simulation results. As shown in Figure 4.8, TIEGeR outperforms GPSR in terms of network lifetime for all the traffic load densities. As discussed above, GPSR tends to choose the same path over and over again. Hence, with increasing load, the network lifetime decreases relative to the increase in the load into the network due to the non-availability of any energy balancing capability. On the contrary, as discussed above, TIEGeR effectively balances out the traffic into the network evenly according to the residual energy levels of the neighbouring nodes in the network. Another peculiar observation similar to the simulation behavior is that with the increase in the load and the number of traffic sources, the nodes close to the destination node tend to get used up more frequently. This behavior is seen as the three independent traffic sources converge at some point and the node where this convergence of the three traffic sources occurs has to deal with the higher traffic passing through it. This leads to lower network lifetime as compared to the cases with lower traffic loads.

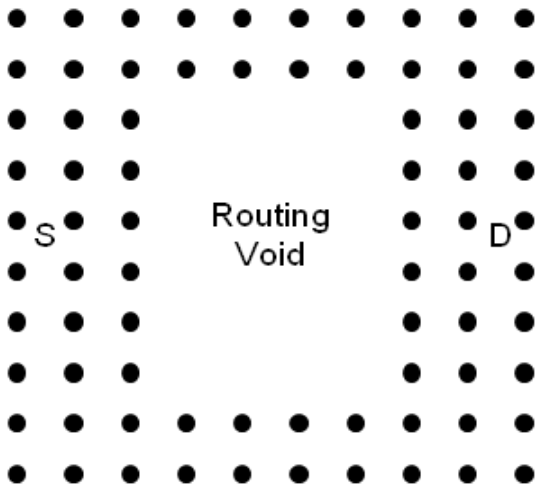

Figure 4.9 Network Scenario 2: Simulation Model (All Static Nodes).

4.3.2 Improvement due to Second-Hop Forward Connectivity Information

The objective of this network scenario is to examine the void handling capabilities of TIEGeR. We consider a large square network topology with a routing void area in the middle of source node S and destination node D (Network Scenario 2) as shown in Figure 4.9 for simulation. In this topology, we begin with only one Source-Destination pair located on the opposite sides of the routing void. The nodes are placed equidistantly and identically in a square with a void area in the middle between the source node S and the destination node D. In other words, there are no forwarding nodes available in the void area to forward the packet towards the destination node using the pure distance based greedy forwarding scheme. The void is specifically and intentionally placed in between the source and the destination nodes in order to monitor the behavior of the routing algorithms while encountering the routing void. This is done to measure the effectiveness of the TIEGeR scheme to predict and avoid the routing void using the additional connectivity information. The shape and size of the routing void is fixed throughout the simulation analysis of the different routing algorithms.

The static source node S sends out CBR data packets at the rate of 45 kbps (corresponding to 50PPS). The simulations are run using three routing algorithms – GPSR, GRR and TIEGeR. In this static network scenario, the goal is to measure

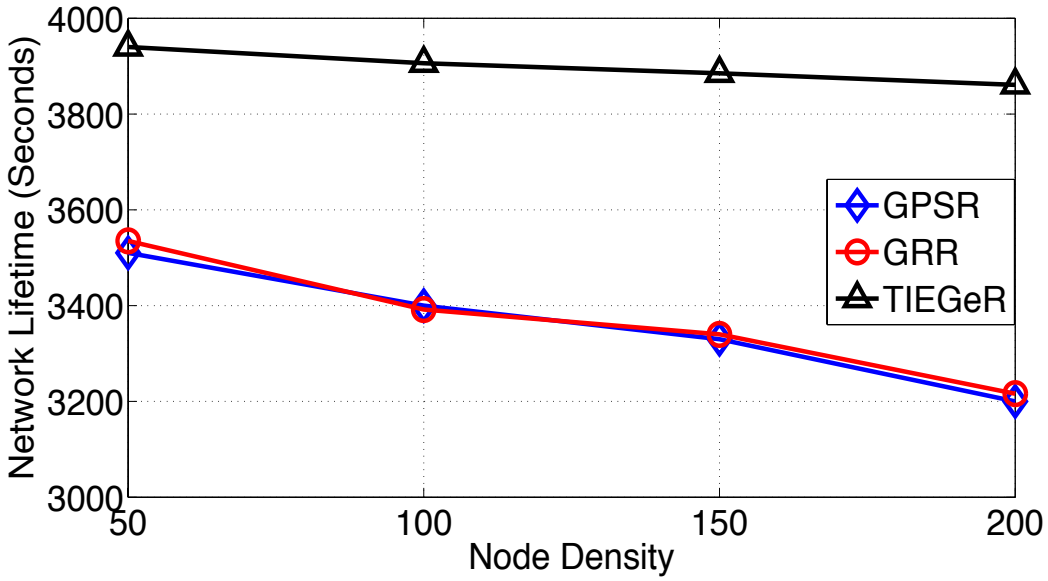

Figure 4.10 Network Lifetime versus Node Density: Simulation Results for Network Scenario 2.

the effect of increasing node density on the performance of the routing algorithms being compared. The simulations are run by gradually increasing the number of nodes in the network from 50 nodes to 200 nodes in steps of 50 nodes. It must be noted that even though the number of nodes in the network is being increased gradually, the overall dimensions of the network are still kept constant. This increases the density of nodes in the network, and not the dimensions of the network. A plot of node density versus the network lifetime is presented in Figure 4.10. It can be seen that throughout the simulation run, for all the node densities simulated, TIEGeR always maintains a higher network lifetime as compared to GPSR and GRR. Moreover the drop in the network lifetime for TIEGeR is less as compared to the GPSR algorithm's network lifetime. This is because GPSR tends to use the same path over the entire duration of the simulation run. Consequently, more energy is consumed on this recurring path being followed for packet transmission as compared to the rest of the nodes in the network. Evidently, this will lead to the nodes along this path to die out faster as compared to the rest of the nodes in the network. Similarly, the connectivity-based GRR also tends to utilize the same static path around the void for all the data packets being

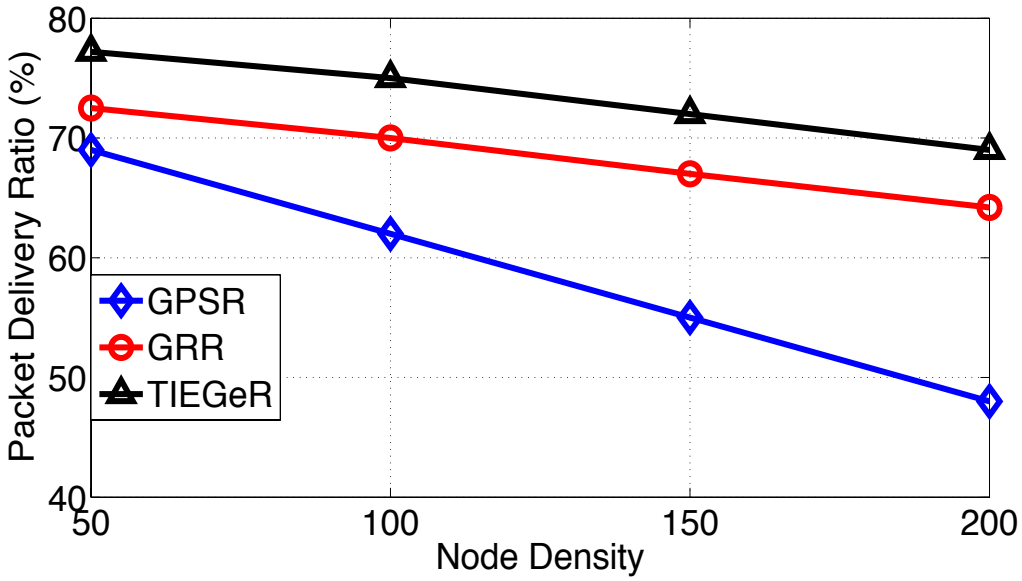

Figure 4.11 Packet Delivery Ratio versus Node Density: Simulation Results for Network Scenario 2.

transmitted. Even though the path followed by the packets transmitted using GRR is not the same as the path for GPSR, both the algorithms lack the ability to use multiple alternate paths around the void, thus lacking any means for energy balancing. TIEGeR actively considers energy balancing by taking the normalized residual energy factor as a contributing element in the routing metric. The effect of such energy balancing is that TIEGeR utilizes many alternative paths to reach the destination node as opposed to a single path taken by all the packets being forwarded by GPSR.

In Figure 4.11, we show the comparison of GPSR, GRR and TIEGeR in terms of the packet delivery ratio. Due to the additional connectivity information, GRR delivers more packets than GPSR. TIEGeR has a higher packet delivery ratio than both GRR and GPSR. Furthermore, the difference in packet delivery ratio between TIEGeR and GPSR increases with increased density in the network. This is due to the increased connectivity leading to predicting and avoiding the "deadlock" nodes. TIEGeR, by using only the *forward progress* nodes to compute the connectivity factor, has the advantage over GRR, which takes into account all

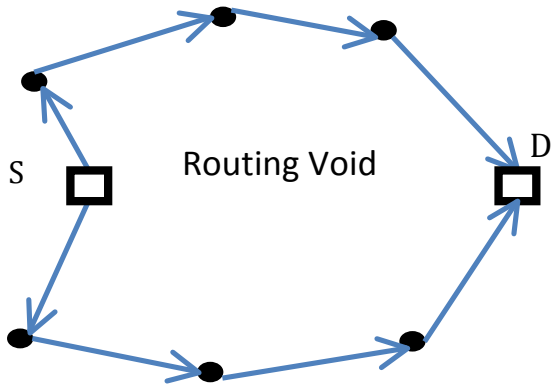

Figure 4.12 Network Scenario 2: Experimental Setup (Routing void between Source and Destination Node).

the neighbour nodes as its connectivity. Hence, TIEGeR is better suited to predict the routing void as compared to GRR, leading to a considerably higher packet delivery ratio. Besides, the multi-parameter *Reverse Progress Mode* enables TIEGeR to still navigate the void in an energy efficient way for lower node density cases.

Again, due to area and hardware limitations, the corresponding experimental setup for Network Scenario 2 shown in Figure 4.12 has the same configuration of Figure 4.9 but with a reduced area and 8 CC2530ZDK WSN nodes, and a routing void present between the source node S and the destination node D. We aim to verify the effectiveness and correctness of the *Reverse Progress Mode* of the TIEGeR algorithm. In order to test the ability of TIEGeR to predict and circumvent the routing void in energy efficient and link aware fashion, we have deliberately placed the source node in such a way that no *Forward Progressing* nodes are available for the source node S. This essentially forces the routing scheme to function in the *reverse progress mode* of the routing algorithm. In this experimental model, the nodes are placed in such a manner that there are two distinct routes across the routing void to the destination node D from the source node S. This forces the source node to begin its routing process in the *reverse progress mode*, thus choosing the next-hop node between the two available paths towards the destination D.

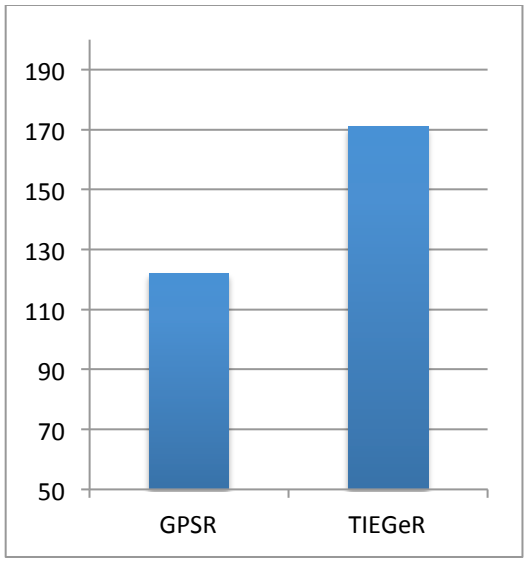

Figure 4.13 Network Lifetime (in Hours): Experimental Results (for Network Scenario 2 of Figure 4.12, and 50 PPS).

Figure 4.13 illustrates the network lifetime (measured in hours) with the source node generating data traffic at the rate of 50 PPS. Even with the presence of the routing void between the source node S and the destination node D, TIEGeR returns around 40% higher network lifetime as compared to GPSR. TIEGeR, even in its *reverse progress* mode, chooses the next-hop based on the residual energy levels as well as the link quality estimates for the next-hop node. On the contrary, GPSR, in its secondary routing mode, tends to use the same path to navigate around the routing void and reach the destination node, thus having a lower network lifetime.

4.3.3 Improvement due to Link Quality Information

In this section, we examine the importance of including link quality information in the routing scheme. Following the trend in network scenarios 1 and 2, we begin with a simulation model of 200m×200m square network with 100 mobile nodes using the random waypoint mobility model, as shown in Figure 4.14. In the random waypoint mobility model, each node travels towards a randomly chosen destination at a speed uniformly distributed between [0, V_{max}]. Upon arrival, the node waits for a certain period of time, called the pause time, before repeating the

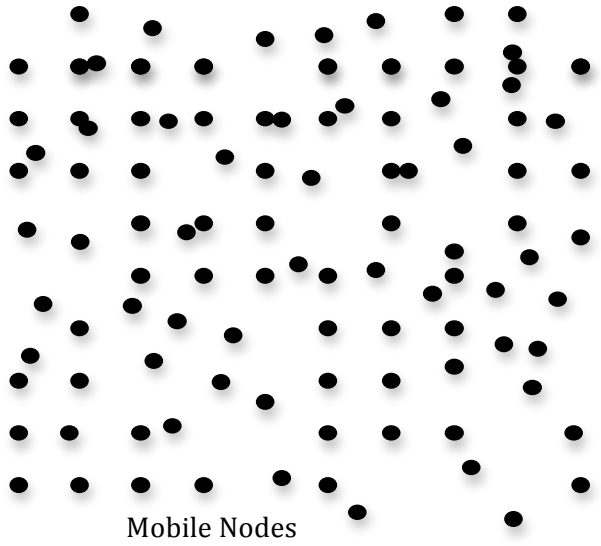

Figure 4.14 Network Scenario 3: Simulation Model.

process again. The objective is to measure the effect of increasing node velocities on the performance of the three routing algorithms being compared, GPSR, PRR*D and TIEGeR.

The simulations are conducted with increasing node velocities and randomly choosing a source-destination pair generating CBR data packet traffic at sufficiently high rate of 45 kbps (or 50PPS), thus avoiding the effects of IEEE 802.15.4 MAC/PHY layers based limitations. The maximum node velocity V_{max} is increased subsequently from 0 to 20 m/s to inspect the limitation of GPSR and PRR*D during high mobility cases. Figure 4.15 presents the plot of packet delivery ratio versus the increasing node velocity V_{max} for the simulation setup in Figure 4.14. GPSR tends to select the node farthest from the current node as the next forwarding hop, but this next-hop might be situated at the circumference of the radio range of the current forwarding node. This leads to higher probability of packet loss due to propagation losses, as the distance between the current node and the candidate node increases and lies around the circumference of the transmission range. Incidentally, if this next forwarding node moves out of the transmission range before the packet is actually transferred to the candidate node, this may lead to packet being dropped. Thus, as seen in Figure 4.15, this leads to

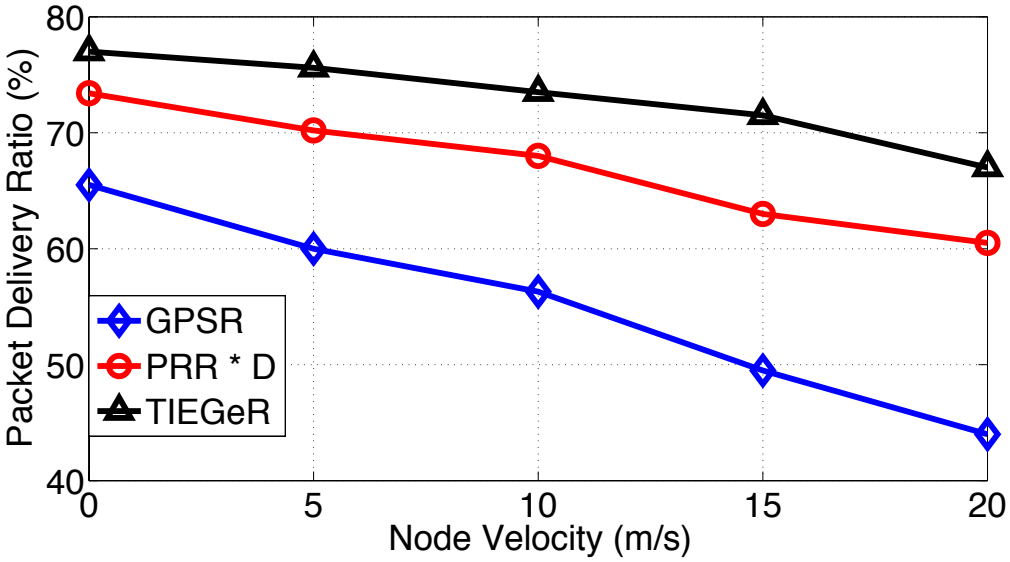

Figure 4.15 Packet Delivery Ratio versus Node Velocity (V_{max}): Simulation Results for Network Scenario 3 (in Figure 4.14) with data rate of 50PPS.

drop in packet delivery ratio for the link quality insensitive geographic routing schemes like GPSR.

On the other hand in TIEGeR, the algorithm tends to select candidate nodes with better link quality, which will lie closer to the current forwarding node as compared to the candidate node selected by GPSR algorithm. Even though PRR*D takes link quality estimation into account, it still selects nodes in the transitional region where the link quality is a highly probabilistic function as compared to the connected region which retains a high link quality index irrespective of the distance. It can be seen that as the node velocity of the nodes increases, TIEGeR substantially outperforms GPSR and PRR*D in terms of PDR. This justifies the notion that link quality is an important routing parameter that considerably affects the overall network behavior.

This is followed by the corresponding experimental setup To further investigate the relevance of Link Quality, we evaluate and compare the performance of GPSR and TIEGeR by both simulations and experiments in a scaled-down static heterogeneous network scenario 4 (shown in Fig. 4.16) using 7 CC2530ZDK

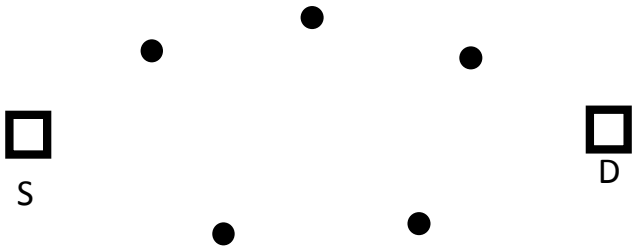

Figure 4.16 Network Scenario 4.

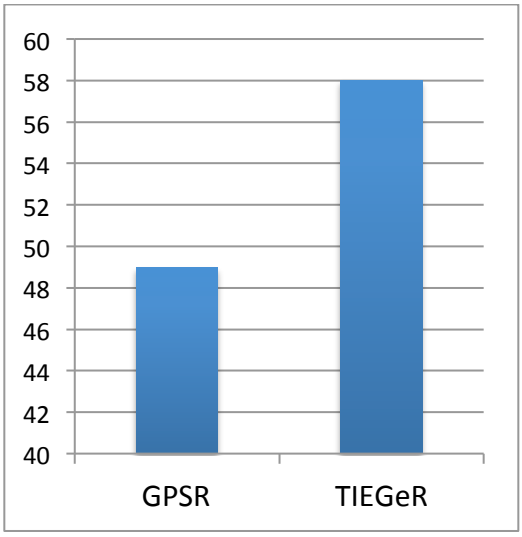

Figure 4.17 Network Lifetime (in Hours): Experimental Result for Network Scenario 4 (in Figure 4.16) and traffic rate of 250 PPS.

WSN nodes, with 5 nodes placed at random between the source and the destination nodes.

Figure 4.17 and Figure 4.18 show the measured results on the network lifetime and packet delivery ratio, corresponding to a data packet rate of 250 PPS, respectively.

As seen from Figure 4.17, the TIEGeR algorithm has a considerably higher network lifetime as compared to GPSR. As discussed earlier, GPSR tends to repeat the path towards the destination node from the source node leading to early powering-out of the nodes along the chosen path, leading to shorter network

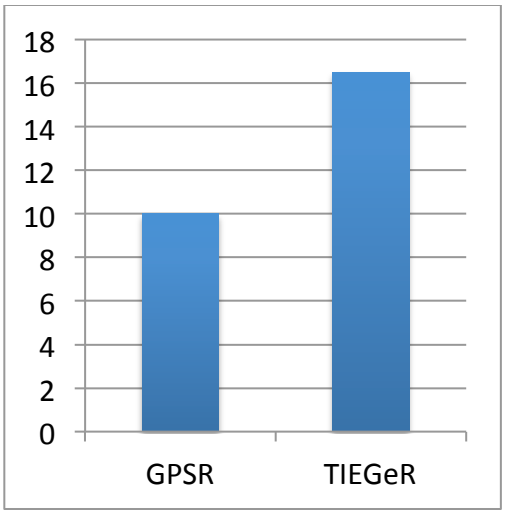

Figure 4.18 Packet Delivery Ratio (in %): Experimental Results for Network Scenario 4 (in Figure 4.16) and traffic rate of 250 PPS.

lifetime. On the other hand, TIEGeR retains a considerably higher network lifetime by effectively routing traffic among multiple nodes in the network.

Moreover, as the nodes along the fixed path for GPSR power out, this leads to drop of packets till the time the powered-out node is removed from the neighbour list of the nodes in the network. Consequently, some packets tend to still be forwarded to the powered-out node, which are dropped on reaching the powered-out node. The behavior of GPSR leads to lower PDR, as evident in Figure 4.18. Also, as GPSR tends to choose the nodes that are farthest away from the current forwarding node towards the destination node, the increased distance between the current node and the next-hop forwarding node translates to lower link quality due to increased propagation losses. Moreover, as the data packet rate of 250 PPS, roughly equal to 240 kbps, is much higher than the IEEE 802.15.4 data throughput limitation of 153 kbps (as previously discussed in Section 4.2.1), the very low packet delivery ratios as seen in Figure 4.18 also inherit the effects of this limitation apart from the other environmental factors such as collisions, propagation loss and CSMA-CA random backoff mechanism.

In order to have a better picture of the PDR performance of the routing algorithms, we conduct both simulations (Figure 4.19) and experiments (Figure

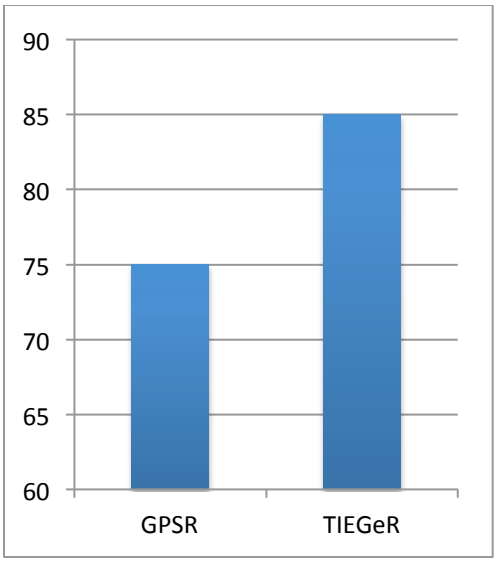

Figure 4.19 Packet Delivery Ratio (in %): Experimental Results for Network Scenario 4 (in Figure 4.16) and traffic rate of 50 PPS.

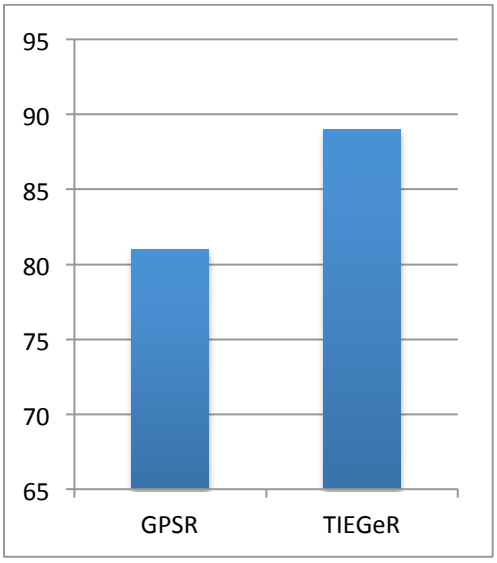

Figure 4.20 Packet Delivery Ratio (in %): Simulation Results for Network Scenario 4 (in Figure 4.16) and traffic rate of 50 PPS.

4.20) with a lower data traffic rate of 50 PPS. As can be seen clearly, the PDR's with 50 PPS in Figures 4.19 and 4.20 are considerably higher than those with 250PPS in Figure 4.18. For the experimental measurements (Figure 4.19), the PDR for the TIEGeR algorithm hovers around 85%, whereas it is 75 % for GPSR.

The same setup in the simulation environment returns the PDR of 81% and 89 % for GPSR and TIEGeR, respectively, as shown in Figure 4.20. The lower PDR for GPSR can be attributed to the increased propagation losses due to the longer distance between the chosen next-hop nodes along the path towards the destination. Evidently, using shorter links along the path towards the destination helps TIEGeR retain a higher PDR as compared to GPSR.

Chapter 5

Conclusions and Future Work

5.1 Thesis Summary

In this thesis, we introduce TIEGeR, a multi-parameter two-hop information based energy efficient Geographic Routing algorithm. TIEGeR, due to its Forward Progress Mode and Reverse Progress Mode, eliminates the need for a dedicated secondary routing algorithm for Geographic Routing schemes. We utilize a combination of Node Link Quality, Distance towards Destination, Node Forward Connectivity and Node Residual Energy Level to compute an energy-efficient and link-aware routing metric. This metric is used by TIEGeR to achieve effective and efficient energy and load balancing among the nodes in the network. Furthermore, the presence of link quality in the routing metric ensures that TIEGeR outperforms other comparable Geographical Routing Schemes including GPSR, PRR*D and GRR in terms of Packet Delivery Ratio. A performance analysis of TIEGeR based on the IEEE 802.15.4 standard specific simulation and experimental results exhibit the performance superiority of TIEGeR in terms of Packet Delivery Rate and Network Lifetime.

In Chapter 3, the models required to formulate the multi-parameter routing metric were discussed. This metric forms the objective function of the TIEGeR algorithm, by incorporating the combined effects of Distance, Link Quality, Connectivity and Residual Energy Level for a comprehensive routing decision. The protocol and implementation details specific to the working of the proposed TIEGeR algorithm were described.

Chapter 4 presented a thorough performance evaluation of TIEGeR based on a combination of simulation and experimental results, highlighting the advantages of TIEGeR over different comparable geographic routing schemes. The chapter started with an evaluation of the IEEE 802.15.4 MAC/PHY layers to identify their

operational limitations. Based on this analysis, it was concluded that the IEEE 802.15.4 standard has an operational threshold of around 150 kbps, and increasing the packet transmission rate beyond this threshold leads to undesirably high packet loss rate. Next, different network scenarios with the simulation and experimental models were implemented to analyse the routing algorithm behaviour. The focus was to highlight the advantage of using node residual energy, forward connectivity and link quality estimates together with node location to return a better routing performance compared to different comparable geographic routing schemes. These results show the superior performance in terms of both Network Lifetime and Packet Delivery Ratio provided by TIEGeR over GPSR and other traditional geographic routing schemes.

5.2 Future Work

In this thesis, we present an energy efficient geographic routing technique that benefits from the additional information collected from the 2-hop neighbourhood of every node. Even though the proposed TIEGeR algorithm outperforms traditional geographic routing schemes, there still is a possibility to further improve the performance of TIEGeR by incorporating more efficient network coding techniques. Furthermore, in TIEGeR, we considered the path-loss model for link quality estimation. While this model can accurately represent the long-term attenuation over the link, it can miss other environmental factors that affect the link quality. Instead, the measured PDR experienced over a link in the past can be continuously updated and used as its quality indicator for consideration in the routing metric. Application of this more proactive link quality estimation criterion in TIEGeR and its potential performance improvement can be another interesting subject for further work.

Appendix A: IEEE 802.15.4 Standard

The IEEE 802.15.4 standard [36-39] was introduced in response to the need for a low-cost, low-power and low rate wireless personal area network (LR-WPAN). The standard was specifically developed keeping in mind the Wireless Sensor Network applications, wherein a number of sensor nodes are deployed. Some of the key characteristics of such WSN nodes are that they have limited battery resources, low range and low bandwidth. The primary application included setting up of ad-hoc networks capable of low-cost and low-power communication among tiny battery powered nodes with little or no support from pre-existing infrastructure. The IEEE 802.15.4 standard defines the PHY and MAC layers, including the channel access mechanism, frame acknowledgement and a network wide association protocol [36-39]. The following sections provide a brief summary of the features of the IEEE 802.15.4 standard.

A.1. An Overview of the IEEE 802.15.4 Standard:

Typical LR-WPAN networks using the IEEE 802.15.4 standard are made up of tiny wireless nodes operating in low-range, low-power networks with a range of up to 10 meters. This network can either operate in a simple one-hop star topology or a more complex self-configuring multi-hop mesh network. A device in an 802.15.4 network can use either a 64-bit IEEE address or a 16-bit short address assigned during the association procedure. The PHY layer utilizes Direct Sequence Spread Spectrum (DSSS) operating in one of the 3 unlicensed ISM (Industrial, Scientific, Medicine) frequency bands:

(i) 868 MHz with 1 channel for a maximum data transfer rate of 20 kbps,

(ii) 915 MHz with 10 channels for a maximum data transfer rate of 40 kbps, and

(iii) 2.4 GHz band with 16 channels for a maximum data transfer rate of 250 kbps.

Furthermore, 802.15.4 embeds the Advanced Encryption Standard (AES) technique for secure data transfer.

The 802.15.4 PHY and MAC layers have been used to develop many upper-layer specifications and standards, including ZigBee, WirelessHART and MiWi. Out of these, ZigBee is the most widespread and popular among vendors and users. ZigBee builds upon the 802.15.4 MAC and PHY layers and adds its own Network layer and Application Profile to develop a low-cost, low-power wireless mesh network standard. On top of the 802.15.4 MAC and PHY layers, ZigBee Standard adds the following components: ZigBee Network Layer (using Simplified AODV routing algorithm), and ZigBee Application Profile (including Application Layer, ZigBee Device Objects (ZDOs) and the custom-built application objects). The complete ZigBee Protocol Stack is illustrated in Figure A.1.

A.2 IEEE 802.15.4 PHY (Physical) Layer

The PHY layer of the 802.15.4 standard provides an interface between the MAC sublayer and the physical radio channel. The PHY layer performs following tasks:

- *Radio Transceiver Activation/Deactivation*: One of the basic responsibilities of the PHY layer is to configure the radio transceiver into one of the three states, namely transmitting, receiving and sleep mode. This is done as per the request generated by the MAC sublayer. During each shift from one state to the other, the amount of time taken by the transceiver is referred to as the turnaround time. This turnaround time is generally not more than 12 symbol periods, where each symbol period roughly equals 16 μs.
- *Energy Detection (ED)*: It is an estimate of the received signal power within the bandwidth of an IEEE 802.15.4 channel. The MAC layer requests this

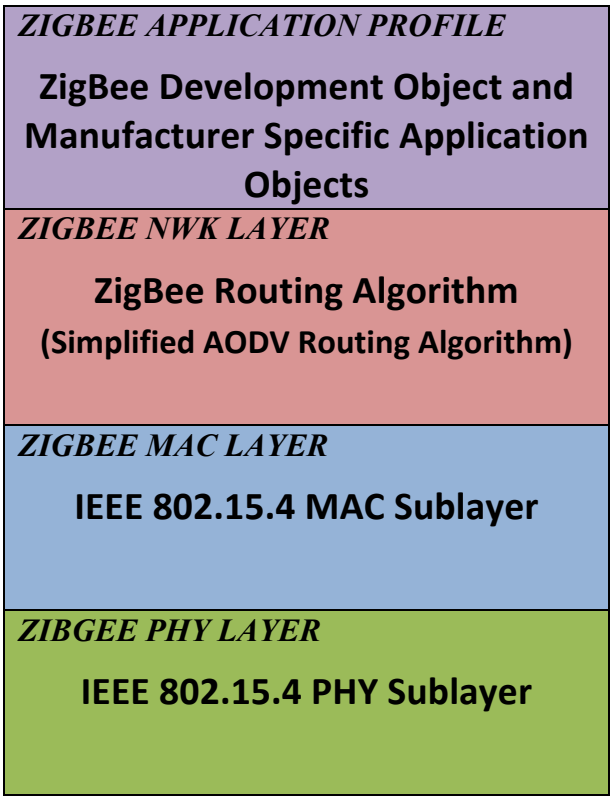

Figure A.1 Protocol Stack Structure for ZigBee.

service and the PHY layer performs the requested tasks and returns the results to the MAC layer. or The result of the ED may be utilized by the MAC layer to perform the clear channel assessment (CCA) with or without the carrier sense functionalities. The energy detection function takes around 8 symbol periods for its operation. The network layer for channel selection algorithms may also use the ED results.

- *Link Quality Indication (LQI)*: Link quality indication measurement is performed for each received packet by the PHY layer. This LQI measurement is performed using the receiver energy detection (ED), signal-to-noise ratio (SNR), or a combination of both ED and SNR to measure the strength and/or quality of a link from which a packet is received.
- *Clear Channel Assessment (CCA) for Carrier Sense Multiple Access with Collision Avoidance (CSMA- CA)*: Before any packet can be transmitted, each node has to ascertain if the channel is free. This is done by the CCA, which is

called by the MAC layer. The PHY layer performs the CCA by utilizing the energy detection, carrier sense, or a combination of these two techniques. In ED mode, the medium is considered busy if any energy above a predefined energy threshold is detected. In carrier sense mode, the medium is considered busy if a signal with the modulation and spreading characteristics of IEEE 802.15.4 is detected. And in the combined mode, both conditions aforementioned need to be met in order to conclude that the medium is busy.

- *Channel Frequency Selection*: The job of the PHY layer is to tune the radio transceiver to a certain channel upon receiving the request from MAC layer. This channel is chosen from the list of relevant channels available to the PHY layer depending on the PHY layer implementation used and the frequency band in which the standard is operating.
- *Data Transmission and Reception*: The PHY layer is also responsible for the implementation of the modulation and spreading techniques utilized by 802.15.4 standard. The 2.4 GHz PHY employs a 16-ary quasi-orthogonal spreading code, in which each group of four information bits is mapped into a 32-chip pseudo-random noise (PN) sequence. The PN sequences for successive data symbols are then concatenated and modulated onto the carrier using offset quadrature phase shift keying (O-QPSK). The 868/915 MHz PHY employs direct sequence spread spectrum (DSSS) with binary phase shift keying (BPSK) used for chip modulation and differential encoding used for data symbol encoding. Each data symbol is mapped into a 15-chip PN sequence and the concatenated PN sequences are then modulated onto the carrier using BPSK with raised cosine pulse shaping.

A.3 IEEE 802.15.4 MAC (Medium Access Control) Layer

The MAC layer provides an interface between the service specific convergence sublayer (SSCS) and the PHY layer. The MAC layer is responsible for the following tasks:

- *Beacon Broadcasts at Coordinator*: A coordinator can determine whether to work in a beacon-enabled mode, in which a superframe structure is used. A coordinator sends out beacons periodically to synchronize the attached devices.
- *Synchronizing to the Beacons*: A device attached to a coordinator operating in a beacon-enabled mode can track the beacons to synchronize with the coordinator. This synchronization is important for data polling, energy saving, and detection of orphaning.
- *Supporting Personal Area Network (PAN) Association and Disassociation*: To support self-configuration, 802.15.4 embeds association and disassociation functions in its MAC sublayer. This not only enables a star to be setup automatically, but also allows for the creation of a self-configuring, peer-to-peer network.
- *Employing the Carrier Sense Multiple Access with Collision Avoidance (CSMA-CA)*: 802.15.4 uses CSMA-CA mechanism for channel access. However, the 802.15.4 standard does away with the request-to-send (RTS) and clear-to-send (CTS) mechanism, in consideration of the low data rate used in LR-WPANs.
- *Guaranteed Time Slot (GTS) Mechanism*: When working in a beacon enabled mode, a coordinator can allocate portions of the active superframe to a device. These portions are called GTSs, and comprise the contention free period (CFP) of the superframe.
- *Link Reliability Between two MAC Entities*: The MAC sublayer employs various mechanisms to enhance the reliability of the link between two peers; among them are the frame acknowledgment and retransmission, data verification by using a 16-bit Cyclic Redundancy Check (CRC), as well as CSMA-CA.

References

[1] N. Xu, "A Survey of Sensor Network Applications.", http://courses.cs.tamu.edu/rabi/cpsc617/resources/sensor%20nw-survey.pdf, *Tech. Report,* USC/Computer Science Department, 2000.

[2] J. Horey, A. Maccabe, "Bosquenet: Studying the Behavior of Porcupines in the Bosque.", http://cs.unm.edu/ jhorey/research/, *Tech. Report*, UNM/Department of Computer Science, 2005.

[3] P. Juang, H. Oki, Y. Wang, M. Martonosi, L.-S. Peh, and D. Rubenstein, "Energy-efficient Computing for Wildlife Tracking: Design Tradeoffs and Early Experiences with Zebranet," in *Proc. Architectural Support for Programming Languages and Operating Systems (ASPLOS-X),* San Jose, pp. 96–107, October 2002.

[4] W.S. Conner, J. Heidemann, L. Krishnamurthy, X. Wang, and M. Yarvis, "Workplace Applications of Sensor Networks.", *Tech. Rep. ISI-TR- 2004-591*, USC/Information Sciences Institute, July 2004.

[5] R. Brooks, P. Ramanathan, and A. Sayeed, "Distributed Target Classification and Tracking in Sensor Networks," in *Proc. IEEE,* 91(8) , pp. 1163-1171, August 2003.

[6] G. Virone, A. Wood, L. Selavo, Q. Cao, L. Fang, T. Doan, Z. He, R. Stoleru, S. Lin, and J. A. Stankovic, "An Assisted Living Oriented Information System based on a Residential Wireless Sensor Network," in *Proc. Distributed Diagnosis and Home Healthcare (D2H2),* pp. 95-100, Arlington, VA, April 2006.

[7] D. Djenouri, and I. Balasingham. "New QoS and Geographical Routing in Wireless Biomedical Sensor Networks," in *Proc. Sixth International Conference on Broadband Communications, Networks, and Systems (BROADNETS 2009)*, Madrid, Spain, pp. 1–8, September 2009.

[8] B. Lichtensteiger, B. Bjelajac, C. Muller, and C. Wietfeld, “RF Mesh Systems for Smart Metering: System Architecture and Performance,” in *Proc. IEEE Smart Grid Communication*, Mayland, USA, Oct. 2010.

[9] S.S.S.R. Depuru, Lingfeng Wang, V. Devabhaktuni, and N. Gudi, "Smart Meters for Power Grid — Challenges, Issues, Advantages and Status," in *Proc Power Systems Conference and Exposition (PSCE), 2011 IEEE/PES*, pp.1-7, March 2011.

[10] B. Karp, and H. T. Kung, “GPSR: Greedy Perimeter Stateless Routing for Wireless Networks,” in *Proc. 6th Annual International Conference on Mobile Computing and Networking (MobiCom)*, Boston, pp. 243–254, 2000.

[11] Takagi, H, and L Kleinrock. “Optimal Transmission Ranges for Randomly Distributed Packet Radio Terminals.” *IEEE Trans. on Communications*, 32(3), pp. 246-257, Mar. 1984.

[12] M. Chen, V.C. Leung, S. Mao, Y. Xiao, and I. Chlamtac, “Hybrid Geographic Routing for Flexible Energy-Delay Tradeoff,” *IEEE Trans. on Vehicular Technology*, 58(9), pp. 4976–4988, Nov. 2009.

[13] S. Basagni, I. Chlamtac, V. R. Syrotiuk, and B. A. Woodward, “A Distance Routing Effect Algorithm for Mobility (DREAM).”, In *Proc. 4th Annual ACM/IEEE International Conference on Mobile Computing and Networking (MobiCom),* Dallas, TX, pp. 76–84, Oct. 1998.

[14] Y. B. Ko and N. H. Vaidya. “Location-aided Routing (LAR) in Mobile Ad Hoc Networks.”, *ACM Wireless Networks,* 6(4), pp. 307-321, July 2000.

[15] G. Finn, “Routing and Addressing Problems in Large Metropolitan-scale Internetworks”, *Tech. Report*, Information Sciences Institute/USC, Virginia, 1988.

[16] I. Stojmenovic and Xu Lin, “Loop-free Hybrid Singlepath/ Flooding Routing Algorithms with Guaranteed Delivery for Wireless Networks”, *IEEE Trans. on Parallel Distribution System*, 12(10), pp. 1023-1032, Oct 2001.

[17] P. Bose, P. Morin, I. Stojmenovic, and J. Urrutia, "Routing with Guaranteed Delivery in Ad Hoc Wireless Networks," in *Proc. 3rd International Workshop on Discrete Algorithms and Methods for Mobile Computing and Communications (DialM '99)*, Aug 1999.

[18] F. Kuhn, R. Wattenhofer, and A. Zollinger. "Worst-Case Optimal and Average-Case Efficient Geometric Ad-Hoc Routing," in *Proc. 4th ACM International Symposium on Mobile Ad Hoc Netowrking and Computing (MobiHoc)*, Annapolis, June 2003.

[19] Y. Yu, R. Govindan, and D. Estrin, "Geographical and Energy Aware Routing: A Recursive Data Dissemination Protocol for Wireless Sensor Networks," *Tech. Rep. UCLA/CSD-TR-01-0023*, Univ. California, Los Angeles, 2001.

[20] A. Dehghani, K. Jamshidi, S. Mirshams, and K. Rahimizadeh. "A Routing Metric for Load Balancing Considering Energy and Delay Constraints in Wireless Sensor Network," in *Proc. International Symposium on Telecommunications (IST 2008)*, Tehran, pp.745-750, Aug 2008.

[21] S. Sharma, H.M. Gupta, and S. Dharmaraja, "EAGR: Energy Aware Greedy Routing Scheme for Wireless Ad Hoc Networks", in *Proc. International Symposium on Performance Evaluation of Computer and Telecommunication Systems (SPECTS 2008)*, Edinburgh, pp. 122 – 129, 2008.

[22] A. Ghaffari, A. Rahmani, and A. Khademzadeh, "Energy-efficient and QoS-aware Geographic Routing Protocol for Wireless Sensor Networks," *Electronics*, 8(8), pp. 582-588, 2011.

[23] H. Huang, G. Hu, and F. Yu, "Energy-aware Multipath Geographic Routing for Detouring Mode in Wireless Sensor Networks," in *Trans. Emerging Telecommunications Technologies*, 22(7), pp. 375-387, Nov. 2011.

[24] S. Lee, B. Bhattacharjee, and S. Banerjee, "Efficient Geographic Routing in Multihop Wireless Networks," in *Proc. 6th ACM International Symposium on Mobile Ad Hoc Networking and Computing (MobiHoc)*, Illinois, pp. 230–241, May 2005.

[25] M. Zuniga, and B. Krishnamachari, “Analyzing the Transitional Region in Low Power Wireless Links,” in *Proc. 1st Annual Conference on Sensor and Ad Hoc Communications and Netowrks (IEEE SECON)*, pp. 517–526, Oct 2004.

[26] K. Seada, M. Zuniga, A. Helmy, and B. Krishnamachari, “Energy Efficient Forwarding Strategies for Geographic Routing in Lossy Wireless Sensor Networks,” in *Proc. 2nd International Conference on Embedded Networked Sensor Systems (Sensys 2004)*, Baltimore, pp. 108–121, Nov 2004.

[27] Eunil Park, and Kwangsu Cho, "Performance Evaluation of Energy Efficient and Reliable Geographic Routing in WSNs," in *Proc. International Conference on Information Science and Applications*, pp. 1-8, 2011.

[28] Kaozhu Dai, Qianping Wang, Wen Xu, Cui Han, Meng Xiong, and Yizhe Cheng, "Link-aware Geographic Routing in WSN," in *Proc. 2010 IEEE 2nd Symposium on Web Society (SWS),* pp.231-236, 16-17 Aug. 2010.

[29] C. Chen, Y. Li, and Y. Song. “An Exploration of Geographic Routing with k-Hop based Searching in Wireless Sensor Networks,” in *Proc. 3rd International Conference on Communications and Networking in China* (*ChinaCom 2008)*, Hangzhou, pp. 376-381, Oct 2008.

[30] M. Li., “Ripple Effect: an Improved Geographic Routing with Local Connectivity Information,” in *Proc. Australian Telecommunication Networks and Applications Conference (ATNAC)*, Adelaide, pp. 252-257, Dec 2008.

[31] H. Liu, J. Wang, X. Zhao, and J. Huang, “Neighbours Investment Geographic Routing Algorithm in Wireless Sensor Networks”, in *Proc. 11th IEEE International Conference High Performance Computing and Commumications (HPCC)*, Seoul, pp. 258-265, July 2009.

[32] G. Calinescu, “Computing 2-hop Neighbourhoods in Ad Hoc Wireless Networks”, in *Proc. AdHoc Mobile and Wireless Networks (AdHocNow 2003)*, Montreal, pp. 175-186, 2003.

[33] T. He, J. A. Stankovic, C. Lu, and T. Abdelzaher, “Speed: A Stateless Protocol for Real-time Communication in Sensor Networks,” in *Proc. International Conference on Distributed Computing Systems (ICDCS)*, pp. 46, May 2003.

[34] Theodore S. Rappapport, *Wireless Communications: Principles and Practice*. Prentice Hall, 2002.

[35] K. Fall, and K. Varadhan, “The NS-Manual”, *Tech. Report*, The VINT Project, Nov. 2008.

[36] J.S. Lee , "Performance Evaluation of IEEE 802.15.4 for Low-rate Wireless Personal Area Networks," *IEEE Trans. on Consumer Electronics*, 52(3), pp.742-749, Aug. 2006.

[37] “Calculating 802.15.4 Data Rates”, Application Note: JN-AN-1035, Jennic, Aug, 2006.

[38] F. Österlind, and A. Dunkels, “Approaching the Maximum 802.15.4 Multihop Throughput”, in *Proc. 5th ACM Workshop on Embedded Networked Sensors (HotEmNets 2008)*, June 2008.

[39] J. Zheng and M.J. Lee, “A Comprehensive Performance Study of IEEE 802.15.4”, *Sensor Network Operations*, IEEE Press, Wiley Interscience, New York, pp. 218–237, 2006.

[40] K. Liu., Personal Research Blog, http://www.cs.binghamton.edu/ kliu, Jan. 2003.